Viscoplastic Fluids: Mathematical Modeling and Applications

Angiolo Farina and Lorenzo Fusi

Abstract Bingham fluids constitute a very important class of non-Newtonian fluids. The modeling of Bingham materials is of crucial importance in industrial applications, since a large variety of materials (e.g. foams, pastes, slurries, oils, ceramics, etc.) exhibit the fundamental character of viscoplasticity, that is the capability of flowing only if the stress is above some critical value. The flow of these materials is difficult to predict, because of the presence of unknown interfaces separating the yielded and the unyielded regions which are difficult to track. This is particularly evident when the flow occurs in complex geometries and when major simplifications, such as lubrication approximation, can be applied. Indeed, in some cases the Bingham model may even lead to a paradox, known as the "lubrication paradox". In this chapter we focus on some practical situations of Bingham flow which are the subject of a current mathematical research (lubrication flows, asymptotic expansions, etc.). Such issues and developments arise, for example, in the petroleum industry and in many natural contexts.

1 Introduction

Bingham fluids, or yield stress fluids, are encountered in a wide range of applications: toothpastes, cements, mortars, foams, muds, mayonnaise, etc. The fundamental character of these fluids is that they are able to deform indefinitely only if they are submitted to a stress above some critical value. Actually, toothpaste

A chapter to appear in "*New trends in non-newtonian fluid mechanics and complex flow*", Lecture Notes Centro Internazionale Matematico Estivo (C.I.M.E.) Series, Lecture Notes in Mathematics, Springer, 2017. The corresponding lectures were given at the CIME-CISM Course "New trends in non-newtonian fluid mechanics and complex flows" held in Levico Terme, Italia, August 28–September 2, 2016

A. Farina (✉) · L. Fusi
Dipartimento di Matematica e Informatica "Ulisse Dini", Firenze, Italy
e-mail: angiolo.farina@unifi.it; lorenzo.fusi@unifi.it

A. Farina et al. (eds.), *Non-Newtonian Fluid Mechanics and Complex Flows*,
Lecture Notes in Mathematics 2212, https://doi.org/10.1007/978-3-319-74796-5_5

visually exhibits the fundamental character of such a fluid model: it flows when the applied stress exceeds a certain value, otherwise it does not flow, behaving as a solid body (actually below the critical stress toothpaste deforms in finite way). Despite the apparent simplicity in the constitutive modeling (especially within the implicit framework theory developed by Rajagopal and co-workers [22–25]), the flow characteristics of these materials are difficult to be predicted, since they involve unknown boundaries separating the liquid and the solid regions. Readers are referred to the books by Huilgol [14] and by Ionescu, Sofonea [15] where several issues concerning the Bingham model (constitutive equations, mathematical techniques, numerical methods and so on) are deeply analyzed.

A well known example of materials which are often modeled as Bingham Fluids are waxy crude oils (i.e. oils with an high paraffin content). These fluids are known to cause handling and pipelining difficulties. The flow properties depend strongly on the yield stress which, in turn, depends on the shear history [31]. This leads to a definable minimum operating point below which flow in a waxy crude oil pipeline would cease.

Familiar examples of non-Newtonian fluids described by the Bingham model include also mud (see [18] and the references therein cited), lubricated pipelining [13], and materials used in ceramic casting [16].

2 Constitutive Model

The simplest shear-stress experiment that characterizes the Bingham fluid is represented in Fig. 1. On the top surface of a layer of material a uniform shear force F is applied. If A is the area of the surface, the applied shear is F/A. If the applied shear load (i.e. force per unit surface) does not exceed a certain threshold, τ_o, the material does not move (the bottom of the layer is fixed on the "floor"). When the applied shear load exceeds the τ_o, the material flows as a linear viscous fluid.

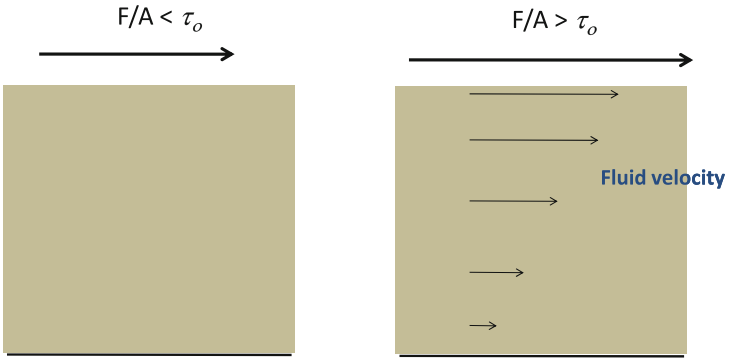

Fig. 1 A schematic representation of the 1D shear stress experiment. F is the shear force and A which is uniformly applied on a surface A so that the shear stress is F/A. The threshold is τ_o

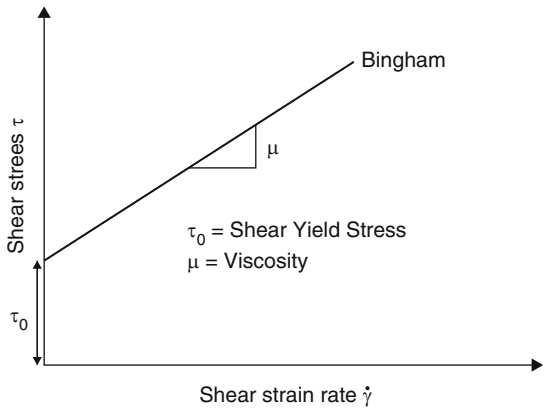

Fig. 2 The shear stress—shear rate curve for the Bingham model

Actually such a peculiar rheological behavior is well highlighted by the experimental tests performed in cylindrical viscometers. We just mention the recent review by Coussot [5] and the numerous experimental papers therein cited. Hence, considering a simple one-dimensional shear flow, if τ denote the modulus of the shear stress and $\dot{\gamma}$ the modulus of the strain rate, the constitutive Bingham model writes as

$$\tau = \tau_o + \mu\dot{\gamma}, \quad \text{if} \quad \tau > \tau_o, \quad \text{(flow)}, \tag{1}$$

and

$$\dot{\gamma} = 0, \quad \text{if} \quad \tau \leq \tau_o, \quad \text{(no flow)}. \tag{2}$$

Indeed (2) means, from the physical point of view, rigid behavior [11]. The threshold τ_o is usually defined shear yield stress, or simply yield stress, and μ is referred to as viscosity. In Fig. 2 we have reported the shear stress-shear rate curve for a Bingham fluid. The model (1), (2) was introduced for the first time by E.C. Bingham [1, 2]. We note that in the Bingham model is much more natural to express the modulus of the shear rate $\dot{\gamma}$ in terms of the modulus of the shear stress τ. Indeed (1), (2) can be rewritten (see also Fig. 3)

$$\dot{\gamma} = \frac{(\tau - \tau_o)_+}{\mu}, \tag{3}$$

where $(\quad)_+$ denotes the positive part, namely

$$(\tau - \tau_o)_+ = \begin{cases} \tau - \tau_o, & \text{if} \quad \tau \geq \tau_o, \\ 0, & \text{if} \quad \tau < \tau_o. \end{cases}$$

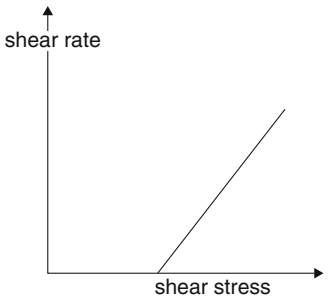

Fig. 3 Shear stress—shear rate according to (3)

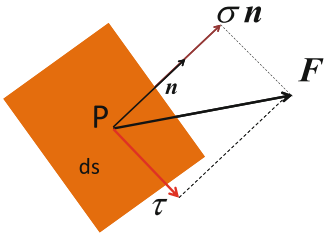

Fig. 4 Decomposition of the force $\boldsymbol{F}$

In the example of Fig. 1 it is easy to identify the shear stress and formulate the yield criterion. But how can we formulate the yield criterion in the general 3D case? What is in this case the shear stress? Let us consider a point P and a small facet of area ds surrounding. The normal to the facet is $\boldsymbol{n}$. If we denote by $\boldsymbol{F}$ the force acting on ds we have

$$\boldsymbol{F} = \mathbf{T}(P)\,\boldsymbol{n},$$

where $\mathbf{T}(P)$ is the Cauchy stress. The force vector $\boldsymbol{F}$ can be splitted into its component along $\boldsymbol{n}$ and in a tangential vector $\boldsymbol{\tau}$ (said tangential or shear force)

$$\boldsymbol{F} = \boldsymbol{\tau} + \sigma \boldsymbol{n},$$

where $\sigma = \boldsymbol{F}\cdot\boldsymbol{n} = \mathbf{T}(P)\,\boldsymbol{n}\cdot\boldsymbol{n}$ (see Fig. 4). Obviously $|\boldsymbol{F}|^2 = \sigma^2 + \tau^2$, where $\tau = |\boldsymbol{\tau}|$. We then consider a reference frame in which $\mathbf{T}(P)$ is diagonal, namely

$$\mathbf{T}(P) = \begin{pmatrix} T_1 & 0 & 0 \\ 0 & T_2 & 0 \\ 0 & 0 & T_3 \end{pmatrix},$$

and assume $T_1 > T_2 > T_3$. Hence

$$|\boldsymbol{F}|^2 = \sigma^2 + \tau^2 = \left| \begin{pmatrix} T_1 & 0 & 0 \\ 0 & T_2 & 0 \\ 0 & 0 & T_3 \end{pmatrix} \begin{pmatrix} n_1 \\ n_2 \\ n_3 \end{pmatrix} \right|^2$$

$$= T_1^2 n_1^2 + T_2^2 n_2^2 + T_3^2 n_3^2,$$

and

$$\begin{aligned}\sigma &= \boldsymbol{F}\cdot\boldsymbol{n} = \mathbf{T}(P)\,\boldsymbol{n}\cdot\boldsymbol{n}\\ &= \begin{pmatrix} T_1 & 0 & 0\\ 0 & T_2 & 0\\ 0 & 0 & T_3\end{pmatrix}\begin{pmatrix} n_1\\ n_2\\ n_3\end{pmatrix}\cdot\begin{pmatrix} n_1\\ n_2\\ n_3\end{pmatrix} = T_1n_1^2 + T_2n_2^2 + T_3n_3^2\,.\end{aligned}$$

We thus get the system

$$\begin{cases} |\boldsymbol{n}|^2 = 1,\\ |\boldsymbol{F}|^2 = \sigma^2+\tau^2,\\ \boldsymbol{F}\cdot\boldsymbol{n} = \sigma,\end{cases}\quad\Longrightarrow\quad\begin{cases} n_1^2+n_2^2+n_3^2 = 1,\\ T_1^2n_1^2+T_2^2n_2^2+T_3^2n_3^2 = \sigma^2+\tau^2,\\ T_1n_1^2+T_2n_2^2+T_3n_3^2 = \sigma,\end{cases}$$

which, once solved with respect to n_1^2, n_2^2, n_3^2, gives

$$\begin{cases} n_1^2 = \dfrac{\left(\sigma-\dfrac{T_2+T_3}{2}\right)^2+\tau^2-\left(\dfrac{T_2-T_3}{2}\right)^2}{(T_2-T_1)(T_3-T_1)} \ge 0,\\ n_2^2 = -\dfrac{\left(\sigma-\dfrac{T_1+T_3}{2}\right)^2+\tau^2-\left(\dfrac{T_3-T_1}{2}\right)^2}{(T_2-T_3)(T_1-T_2)} \ge 0,\\ n_3^2 = \dfrac{\left(\sigma-\dfrac{T_2+T_1}{2}\right)^2+\tau^2-\left(\dfrac{T_2-T_1}{2}\right)^2}{(T_1-T_3)(T_2-T_3)} \ge 0.\end{cases}$$

Thus, in the (σ,τ) plane a domain is defined

$$\begin{aligned}\left(\sigma-\frac{T_2+T_3}{2}\right)^2+\tau^2 &\ge \left(\frac{T_2-T_3}{2}\right)^2,\\ \left(\sigma-\frac{T_1+T_3}{2}\right)^2+\tau^2 &\le \left(\frac{T_3-T_1}{2}\right)^2,\\ \left(\sigma-\frac{T_2+T_1}{2}\right)^2+\tau^2 &\ge \left(\frac{T_2-T_1}{2}\right)^2,\end{aligned}$$

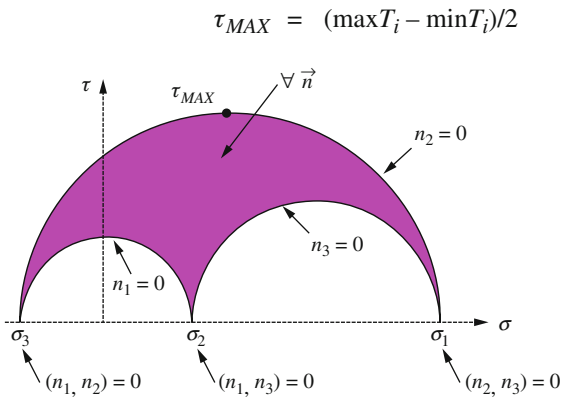

Fig. 5 Three points on the horizontal axis correspond to the three main stresses. The figure shows that the maximum shear is equal to the radius of the largest circle

which corresponds to the area bordered by three circles, the so-called three Mohr circles (see Fig. 5). Thus, since the maximum shear stress is τ_{MAX}, a possible yield criterion is

$$\begin{cases} \tau_{MAX} \leq \dfrac{\tau_o}{2}, & \text{no flow,} \\ \\ \tau_{MAX} > \dfrac{\tau_o}{2}, & \text{flow,} \end{cases} \tag{4}$$

where

$$\tau_{MAX} = \frac{1}{2} \max \left\{ |T_1 - T_2|\,,\ |T_2 - T_3|\,,\ |T_3 - T_1| \right\}. \tag{5}$$

Such a criterion is known as Tresca criterion [3]. The representation in the principal stress space of the surface (5), known as Tresca Surface, or

$$\left[(T_1 - T_2)^2 - \tau_o^2 \right] \left[(T_1 - T_3)^2 - \tau_o^2 \right] \left[(T_3 - T_2)^2 - \tau_o^2 \right] = 0,$$

is a cylindrical unbounded surface with hexagonal section and axis (1,1,1). So, according to the Tresca criterion, at every point of the material we have to compute the eigenvalues of the stress tensor. If all the eigenvalues are within the Tresca surface then the material is in a rigid state. if at least one of the eigenvalues is outside the surface then the material is in a fluid state.

The Tresca criterion, unfortunately, is not very practical to use. For this reason it is preferred to use the Von Mises criterion [30], based on the second invariant of the stress tensor. The maximum shear stress criterion (4) is replaced by

$$\begin{cases} \tau_{VM} \leq \dfrac{\tau_o}{2}, & \text{no flow,} \\ \\ \tau_{VM} > \dfrac{\tau_o}{2}, & \text{flow,} \end{cases}$$

where

$$\tau_{VM} = \sqrt{\frac{1}{2}\left[(T_1 - T_2)^2 + (T_2 - T_3)^2 + (T_3 - T_1)^2\right]}.$$

Thus, splitting the Cauchy stress as $\mathbf{T} = -P\mathbf{I} + \mathbf{S}$, where $P = 1/3\text{tr}\mathbf{T}$ and $\mathbf{S}$ is the extra-stress, we immediately realize that σ_{VM} coincides with the second invariant of the extra-stress, namely

$$\sigma_{VM} = II_{\mathbf{S}} = \sqrt{\frac{1}{2}\text{tr}\,\mathbf{S}^2}.$$

Therefore the generalization of the Bingham model (1), (2) to the 3D case is the following

$$\mathbf{S} = \left(2\mu + \frac{\tau_o}{II_{\mathbf{D}}}\right)\mathbf{D}, \quad \text{if} \quad II_{\mathbf{S}} > \tau_o, \quad \text{(flow)}, \tag{6}$$

and

$$\mathbf{D} = 0, \quad \text{if} \quad |\tau| \leq \tau_o, \quad \text{(no flow)}, \tag{7}$$

where

$$\mathbf{D} = \frac{1}{2}\left(\nabla \boldsymbol{v} + \nabla \boldsymbol{v}^{\text{T}}\right) \qquad II_{\mathbf{D}} = \sqrt{\frac{1}{2}\,\text{tr}\,\mathbf{D}},$$

and where $\boldsymbol{v}$ is the fluid velocity field. We remark that the Bingham constitutive equation can be written in the implicit form (see [22–24, 26])

$$\mathbf{D} = \left(\frac{II_{\mathbf{D}}}{2\mu II_{\mathbf{D}} + \tau_o}\right)\mathbf{S}. \tag{8}$$

The above constitutive equation allows to express $\mathbf{S}$ as a function of $\mathbf{D}$ only when $II_{\mathbf{S}} > \tau_o$, while $\mathbf{D} = 0$, entails only $II_{\mathbf{S}} \leq \tau_o$, the stress being constitutively undetermined.

3 Flow in a Channel

We consider the flow of an incompressible Bingham fluid in a symmetric channel of length L and width $2H$. We consider a laminar flow so that the velocity field is

$$\boldsymbol{v} = v(y, t)\boldsymbol{e}_x,$$

where, as shown in Fig. 6, x, y are the longitudinal and transversal coordinates respectively. Due to symmetry we consider just the upper part of the channel. The the inlet pressure ΔP is prescribed and we rescale the outlet pressure to 0. Hence

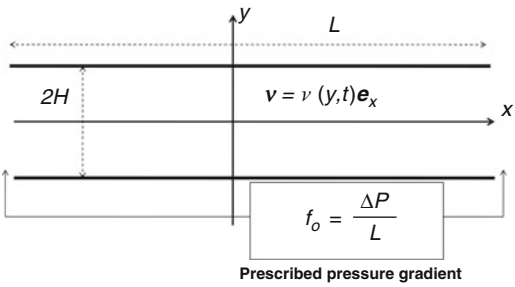

Fig. 6 Sketch of the channel

the pressure gradient driving the flow is given by

$$f_o = \frac{\Delta P}{L}\,.$$

In principle $f_o = f_o\,(t)$ since ΔP may depend on time. In such a simple setting

$$\mathbf{D} = \begin{pmatrix} 0 & v_y & 0 \\ v_y & 0 & 0 \\ 0 & 0 & 0 \end{pmatrix}, \qquad \mathbf{T} = \begin{pmatrix} -P & S_{12} & 0 \\ S_{12} & -P & 0 \\ 0 & 0 & -P \end{pmatrix},$$

so that $II_{\mathbf{S}} = |S_{12}|$ and $II_{\mathbf{D}} = \left|v_y\right|$. Hence, (6), (7) give

$$II_{\mathbf{S}} > \tau_o, \quad \Longrightarrow \quad S_{12} = -\tau_o + \mu v_y,$$

$$II_{\mathbf{S}} \leq \tau_o, \quad \Longrightarrow \quad v_y = 0.$$

Next, we assume that the viscous region, namely $II_{\mathbf{S}} > \tau_o$, and the rigid region, $II_{\mathbf{S}} \leq \tau_o$, are separated by a sharp interface $y = s(t)$ a priori unknown, i.e. a free boundary. In the fluid region, i.e. $s\,(t) < y < H$, the motion equation reduces to

$$\rho v_t = \mu v_{yy} + f_o,$$

coupled with the no-slip condition on $y = H$,

$$v\,(H, t) = 0,$$

and with the threshold condition on the free boundary $s\,(t)$

$$S_{12}|_{y=s} = \tau_o, \quad \Longrightarrow \quad v_y\,\big|_{y=s} = 0.$$

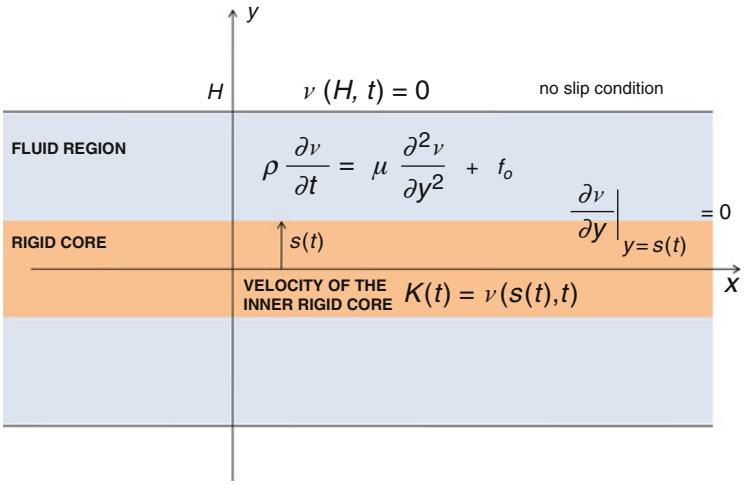

Fig. 7 The position $s(t)$ of the "fluid – rigid" is unknown. Indeed we deal with a free boundary problem

In particular, we assume no-slip also at the interface $s\,(t)$, so that the velocity of the rigid core is

$$\kappa\,(t) = v\,(s\,(t)\,,t)\,.$$

Figure 7 represents a sketch of the problem we have to solve. We need an evolution for the interface $s\,(t)$. According to the approach developed in [12], which is based on the pioneering works by Safronchik [29] and Rubinstein [28], the unyielded region is treated as an evolving non material volume, whose motion is determined by using the integral (or global) momentum balance. The dynamics of the unyielded domain

$$\Omega\,(t) = \{0 < x < L,\ \ -s\,(t) < y < s\,(t)\}\,,$$

is thus given by (see, e.g., [3])

$$\frac{d}{dt}\int_{\Omega(t)} \rho \boldsymbol{v} dV = \int_{\partial\Omega(t)} \mathbf{T}\boldsymbol{n}\, dS - \int_{\partial\Omega(t)} \rho \boldsymbol{v}\,[(\boldsymbol{v}-\boldsymbol{w})\cdot\boldsymbol{n}]\, dS, \tag{9}$$

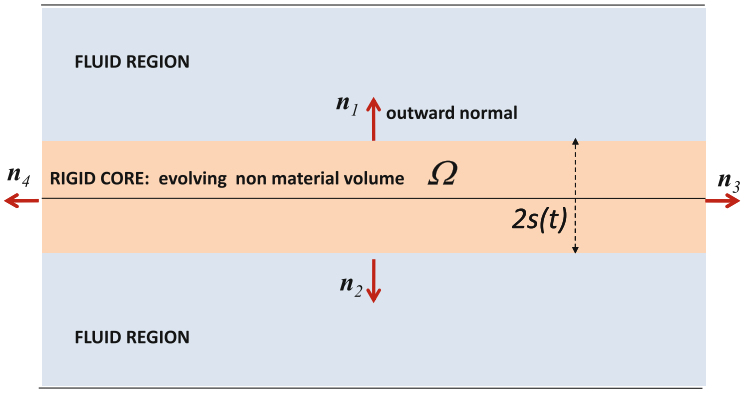

Fig. 8 The evolving non-material domain Ω

where $\boldsymbol{w}$ is the velocity of the boundary[1] $\partial\Omega$ and $\boldsymbol{n}$ its outward normal. Taking Fig. 8 into account relation (9) reduces to[2]

$$v_t\left(s\left(t\right),t\right)=\frac{1}{\rho}\left(f_o-\frac{\tau_o}{s\left(t\right)}\right).$$

We thus end up with this free boundary problem

$$\begin{cases}\rho v_t=\mu v_{yy}-f_o, & s\left(t\right)<y<H,\ t>0\\ v\left(H,t\right)=0, & t>0,\\ v_y\left(s\left(t\right),t\right)=0, & t>0,\\ \rho v_t\left(s\left(t\right),t\right)=f_o-\dfrac{\tau_o}{s\left(t\right)}, & t>0,\\ v\left(y,0\right)=v_o\left(y\right) & 0<y<s_o,\\ s\left(0\right)=s_o.\end{cases}\tag{10}$$

The domain of the problem is represented in Fig. 9. The problem (10) is a free boundary problem but not of Stefan type, because in the evolution equation for the free boundary $\dot{s}$ does not appear. However if we consider as new dependent variable

[1] In the 1D case, considering just the upper part of Ω, $\boldsymbol{w}=\dot{s}\left(t\right)\boldsymbol{e}_y$.

[2] We remark that $\dot{\kappa}\left(t\right)\neq v_t\left(s\left(t\right),t\right)$.

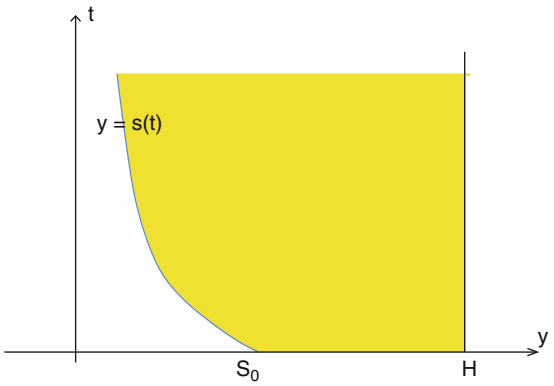

Fig. 9 Sketch of the domain of problem (10)

$z\,(y.t) = v_t\,(y,t)$, problem (10) rewrites as

$$\begin{cases} \rho z_t = \mu z_{yy}, & s\,(t) < y < H,\ t > 0 \\ z\,(H,t) = 0, & t > 0, \\ \rho z\,(s\,(t)\,,t) = f_o - \dfrac{\tau_o}{s\,(t)}, & t > 0, \\ z_y\,(s\,(t)\,,t) = \dfrac{\tau_o}{s\,(t)}\dot{s}, & t > 0, \\ v\,(y,0) = v_o\,(y) & 0 < y < s_o, \\ s\,(0) = s_o. \end{cases} \tag{11}$$

In [4] global well posedness of problem (11) has been proved.

4 Bingham Model with Deformable Core

The Bingham model predicts that the material behaves as a rigid body if the shear stress is less than the threshold τ_o. It is however evident that the schematization of the rigid body is not plausible from a physical point of view (think, for example, to the mayonnaise). Oldroyd [20] and Yoshimura et al. [32] have proposed to treat the "solid phase" as deformable. In [7] Fusi et al. have studied an extension of the 1D problem (10) to the case of an elastic core. The model has been developed within the context of the theory of natural configurations [24, 25]. In [10] Fusi et al. have extended the problem studied in [7] to a 2D channel flow where the channel amplitude is not uniform.

Actually, other models have been proposed for Bingham-like fluids whose unyielded core is deformable. In [8, 9], for instance, the material in the non-fluid region has been modeled as a visco-elastic fluid.

4.1 Channel Flow of a Bingham-Like Fluid with Linear Elastic Core

Here we consider a channel flow of a Bingham-like fluid driven by a known pressure gradient, assuming that the continuum behaves as a linear viscous fluid if the stress is above the yield stress and as a linear elastic solid when the stress is below such a threshold. In particular we assume that the domain may be split in two sub-domains, see Fig. 10. The inner core, in which the material behaves as a linear elastic material, and the outer part (i.e. the one close to the channel walls) where a linear viscous behavior occurs. The two regions are separated by the unknown sharp interfaces $y = \pm\sigma(x, t)$. Moreover the channel width varies along x, so that the channel walls are given by the function $y = H(x)$. The channel is finite and we denote its length by L. As in Sect. 3, we limit our analysis to the upper part of the channel because of symmetry. The motion equations are obtained by imposing the mass and momentum balance. The evolution equation of the interface $y = \sigma(x, t)$, as well as the boundary conditions, are derived imposing Rankine-Hugoniot conditions and Von Mises yield criterion. The general mathematical problem is therefore a two-dimensional free boundary problem. We develop the model assuming that the characteristic height of the upper part H is far less than L, i.e. the aspect ratio

$$\varepsilon = \frac{H}{L} \ll 1$$

is very small.

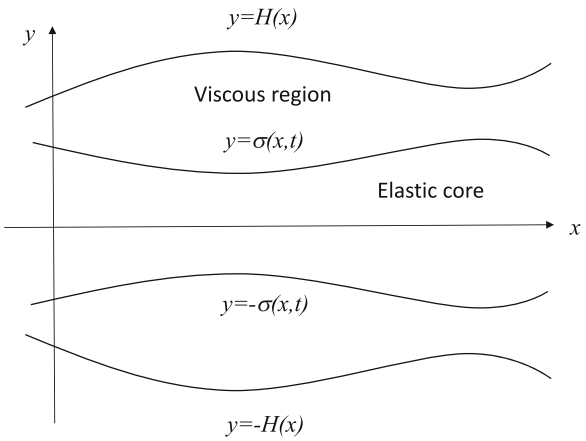

Fig. 10 A schematic representation of the channel flow with deformable core

4.2 Kinematics and Constitutive Equation

Consider a two dimensional setting and assume that the motion is given by

$$\boldsymbol{x} = \boldsymbol{\chi}\ (\boldsymbol{X}, t), \tag{12}$$

where $\boldsymbol{\chi}$ is a differentiable and invertible mapping from $\mathbf{R}^2 \rightarrow \mathbf{R}^2$. The vectors $\boldsymbol{x}$, $\boldsymbol{X}$ are the Eulerian and Lagrangian coordinates, respectively. The deformation tensor is[3]

$$\mathbf{F} = \text{grad}\boldsymbol{\chi}\ (\boldsymbol{X}, t)$$

and mechanical incompressibility entails $\det \mathbf{F} = 1$.The Eulerian velocity and acceleration are defined as

$$\boldsymbol{v}\ (\boldsymbol{x}, t) = \left.\frac{\partial \boldsymbol{\chi}}{\partial t}\right|_{\boldsymbol{X}=\boldsymbol{\chi}^{-1}(\boldsymbol{x},t)}$$

$$\boldsymbol{a}\ (\boldsymbol{x}, t) = \left.\frac{\partial^2 \boldsymbol{\chi}}{\partial t^2}\right|_{\boldsymbol{X}=\boldsymbol{\chi}^{-1}(\boldsymbol{x},t)}$$

respectively. The strain rate tensor is

$$\mathbf{D} = \begin{pmatrix} \dfrac{\partial v_1}{\partial x} & \dfrac{1}{2}\left(\dfrac{\partial v_1}{\partial y} + \dfrac{\partial v_2}{\partial x}\right) \\ \dfrac{1}{2}\left(\dfrac{\partial v_1}{\partial y} + \dfrac{\partial v_2}{\partial x}\right) & \dfrac{\partial v_2}{\partial y} \end{pmatrix},$$

and mechanical incompressibility gives

$$\text{tr}\,\mathbf{D} = \frac{\partial v_1}{\partial x} + \frac{\partial v_2}{\partial y} = 0. \tag{13}$$

Splitting, as usual, the Cauchy stress as $\mathbf{T} = -P\mathbf{I} + \mathbf{S}$, with $P = 1/3\text{tr}\mathbf{T}$, we extend we extend the constitutive relation (6), (7) to the case in which the region $II_{\mathbf{S}} < \tau_o$ behaves as a linear elastic material[4] (see [7, 10]).

$$\left[\mathbf{S} - \left(2\mu + \frac{\tau_o}{II_{\mathbf{D}}}\right)\mathbf{D}\right] \Theta\ (II_{\mathbf{S}} - \tau_o) + (\mathbf{S} - 2\eta\mathbf{E})\ \Theta\ (\tau_o - II_{\mathbf{S}}) = 0, \tag{14}$$

[3]Here grad denotes the gradient operator w.r.t. Lagrangian coordinates, while ∇ the gradient w.r.t. Eulerian coordinates.

[4]We are considering a linear elastic model even if $\|\mathbf{F}\|$ may be, in general, not very "small" , as we shall see in Sect. 4.3.3.

where

$$\mathbf{E} = \frac{1}{2}\left[\nabla \boldsymbol{f} + (\nabla \boldsymbol{f})^{\mathrm{T}}\right]$$

is the linearized strain tensor, $\boldsymbol{f} = \boldsymbol{\chi} - \boldsymbol{X}$ is the displacement , η is the elastic modulus and Θ is the Heaviside function

$$\Theta(z) = \begin{cases} 0, \text{ if } z < 0, \\ \\ 1, \text{ if } z \geqslant 0. \end{cases}$$

From (14) it is clear that, whenever $II_{\mathbf{S}} \leq \tau_o$, the continuum behaves as a linear elastic solid whereas the viscous behavior occurs when $II_{\mathbf{S}} \geq \tau_o$.

4.3 Flow in a Channel

We rescale the longitudinal variable as

$$\tilde{x} = \frac{x}{L} \qquad \tilde{h}(x) = \frac{H(x)}{H} \qquad \tilde{\sigma} = \frac{\sigma}{H} \qquad H = \max_{x \in [0,L]} H(x)$$

and we introduce the Reynolds and Bingham number

$$\mathsf{Re} = \frac{\rho U H}{\mu}, \quad \mathsf{Bn} = \frac{\tau_o H}{\mu U}, \tag{15}$$

where U is the characteristic velocity and ρ is the material density. The we set

$$\tilde{y} = \frac{1}{\varepsilon}\frac{y}{L} \qquad \tilde{t} = \frac{t}{t_c} \qquad t_c = \frac{L}{U}.$$

Concerning velocity and pressure, we introduce

$$\tilde{v}_1 = \frac{v_1}{U}, \quad \tilde{v}_2 = \frac{v_2}{\varepsilon U}, \quad \tilde{P} = \frac{P}{P_c} \quad P_c = \frac{\mu U L}{H^2}$$

where P_c comes from the classical Poiseuille formula. Rescaling $\mathbf{S}$ as

$$\mathbf{S} = \frac{\mu U}{H}\begin{pmatrix} \tilde{S}_{11} & \tilde{S}_{12} \\ \\ \tilde{S}_{12} & \tilde{S}_{22} \end{pmatrix},$$

the motion equations become[5]

$$\frac{\mathrm{Re}}{\varepsilon}\left(\frac{\partial v_1}{\partial t}+\frac{\partial v_1}{\partial x}v_1+\frac{\partial v_1}{\partial y}v_2\right)=-\frac{1}{\varepsilon^2}\frac{\partial P}{\partial x}+\frac{1}{\varepsilon}\frac{\partial}{\partial x}\left(S_{11}\right)+\frac{1}{\varepsilon^2}\frac{\partial}{\partial y}\left(S_{12}\right), \tag{16}$$

$$\frac{\mathrm{Re}}{\varepsilon}\left(\frac{\partial v_2}{\partial t}+\frac{\partial v_2}{\partial x}v_1+\frac{\partial v_2}{\partial y}v_2\right)=-\frac{1}{\varepsilon^4}\frac{\partial P}{\partial y}+\frac{1}{\varepsilon^2}\left[\frac{\partial}{\partial x}\left(S_{12}\right)+\frac{1}{\varepsilon}\frac{\partial}{\partial y}\left(S_{22}\right)\right], \tag{17}$$

and mass conservation is

$$\frac{\partial v_1}{\partial x}+\frac{\partial v_2}{\partial y}=0. \tag{18}$$

The displacement is rescaled as

$$\tilde{f}_1=\frac{f_1}{L}\qquad \tilde{f}_2=\frac{1}{\varepsilon}\frac{f_2}{L},$$

so that[6]

$$\mathbf{E}=\begin{pmatrix}\dfrac{\partial f_1}{\partial x} & \dfrac{1}{2}\left(\dfrac{1}{\varepsilon}\dfrac{\partial f_1}{\partial y}+\varepsilon\dfrac{\partial f_2}{\partial x}\right)\\ \dfrac{1}{2}\left(\dfrac{1}{\varepsilon}\dfrac{\partial f_1}{\partial y}+\varepsilon\dfrac{\partial f_2}{\partial x}\right) & \dfrac{\partial f_2}{\partial y}\end{pmatrix}.$$

The sharp interface $y=\sigma(x,t)$ separates the elastic domain from the viscous domain, as shown in Fig. 2. We remark that the interface σ is unknown and it is not material. The dimensionless normal velocity of the interface is

$$w=\frac{\varepsilon}{\sqrt{1+\varepsilon^2\left(\dfrac{\partial\sigma}{\partial x}\right)^2}}\frac{\partial\sigma}{\partial t}.$$

The dimensionless strain rate tensor is

$$\mathbf{D}=\begin{pmatrix}\varepsilon\dfrac{\partial v_1}{\partial x} & \dfrac{1}{2}\left(\dfrac{\partial v_1}{\partial y}+\varepsilon^2\dfrac{\partial v_2}{\partial x}\right)\\ \dfrac{1}{2}\left(\dfrac{\partial v_1}{\partial y}+\varepsilon^2\dfrac{\partial v_2}{\partial x}\right) & \varepsilon\dfrac{\partial v_2}{\partial y}\end{pmatrix},$$

[5]We omit "˜" to keep notation simple.

[6]Again, we have omitted " ".

while the dimensionless invariant $II_{\mathbf{D}}$ is

$$II_{\mathbf{D}} = \frac{1}{2}\sqrt{\left(\frac{\partial v_1}{\partial y} + \varepsilon^2 \frac{\partial v_2}{\partial x}\right)^2 + 2\varepsilon^2 \left[\left(\frac{\partial v_1}{\partial x}\right)^2 + \left(\frac{\partial v_2}{\partial y}\right)^2\right]}. \tag{19}$$

The yield criterion becomes

$$II_{\mathbf{S}} \lesseqgtr \mathsf{Bn}. \tag{20}$$

4.3.1 Boundary Conditions

Let $[\![\cdot]\!]$ denotes the "jump" across the surface $y = \sigma$. Assuming no-slip on σ we get

$$[\![v_1]\!] = [\![v_2]\!] = 0. \tag{21}$$

The continuity of the stress gives

$$-[\![P]\!]\left(1 + \varepsilon^2 \left(\frac{\partial \sigma}{\partial x}\right)^2\right) + \left[\!\!\left[\varepsilon^3 S_{11} \left(\frac{\partial \sigma}{\partial x}\right)^2 - 2\varepsilon^2 S_{12} \frac{\partial \sigma}{\partial x} + \varepsilon S_{22} \right]\!\!\right] = 0, \tag{22}$$

and

$$[\![S_{12}]\!] + \varepsilon \frac{\partial \sigma}{\partial x}\left[\!\!\left[S_{22} - S_{11} - \varepsilon S_{12} \frac{\partial \sigma}{\partial x} \right]\!\!\right] = 0. \tag{23}$$

Remark 1 If we neglect $\mathscr{O}(\varepsilon)$ terms, then $[\![P]\!] = [\![S_{12}]\!] = 0$, provided that S_{ij} are bounded.

On the channel wall $y = h$ the no-slip condition yields $\boldsymbol{v}(x, h, t) \equiv 0$, while the boundary conditions for the pressure are

$$P(0, y, t) = P_{in}(t), \quad \text{and} \quad P(1, y, t) = P_{in}(t) - \Delta P(t), \quad \text{with} \ \Delta P \geq 0.$$

Finally, we impose the symmetry conditions:

$$\frac{\partial f_1(x, 0, t)}{\partial y} = 0, \qquad f_2(x, 0, t) = 0, \qquad \frac{\partial f_2(x, 0, t)}{\partial y} = 0, \qquad \frac{\partial f_2(x, 0, t)}{\partial t} = 0. \tag{24}$$

4.3.2 The Elastic Domain and the Viscous Domain

Let us first consider the elastic domain $y \in [0, \sigma]$. According to (14)

$$\mathbf{S} = \frac{\mathsf{Re}}{\lambda^2} \begin{pmatrix} 2\dfrac{\partial f_1}{\partial x} & \dfrac{1}{\varepsilon}\dfrac{\partial f_1}{\partial y} + \varepsilon \dfrac{\partial f_2}{\partial x} \\ \dfrac{1}{\varepsilon}\dfrac{\partial f_1}{\partial y} + \varepsilon \dfrac{\partial f_2}{\partial x} & 2\dfrac{\partial f_2}{\partial y} \end{pmatrix},$$

with

$$\lambda^2 = \left(\frac{U}{c}\right)^2 \qquad c^2 = \frac{\eta}{\rho}. \tag{25}$$

The momentum balance yields

$$\begin{aligned} &\mathsf{Re}\left(\frac{\partial^2 f_1}{\partial t^2} + \frac{\partial^2 f_1}{\partial x \partial t}\frac{\partial f_1}{\partial t} + \frac{\partial^2 f_1}{\partial y \partial t}\frac{\partial f_2}{\partial t}\right) \\ &\quad = -\frac{1}{\varepsilon}\frac{\partial P}{\partial x} + \frac{\mathsf{Re}}{\lambda^2}\left(2\frac{\partial^2 f_1}{\partial x^2} + \frac{1}{\varepsilon^2}\frac{\partial^2 f_1}{\partial y^2} + \frac{1}{\varepsilon}\frac{\partial^2 f_2}{\partial y \partial x}\right), \end{aligned} \tag{26}$$

$$\begin{aligned} &\mathsf{Re}\left(\frac{\partial^2 f_2}{\partial t^2} + \frac{\partial^2 f_2}{\partial x \partial t}\frac{\partial f_1}{\partial t} + \frac{\partial^2 f_2}{\partial y \partial t}\frac{\partial f_2}{\partial t}\right) \\ &\quad = -\frac{1}{\varepsilon^3}\frac{\partial P}{\partial y} + \frac{\mathsf{Re}}{\lambda^2}\left(\frac{1}{\varepsilon^2}\frac{\partial^2 f_1}{\partial x \partial y} + \frac{\partial^2 f_2}{\partial x^2} + \frac{2}{\varepsilon^2}\frac{\partial^2 f_2}{\partial y^2}\right). \end{aligned} \tag{27}$$

In the viscous domain $y \in [\sigma, 1]$

$$\mathbf{S} = \left(1 + \frac{\mathsf{Bn}}{2II_{\mathbf{D}}}\right) \begin{pmatrix} 2\varepsilon\dfrac{\partial v_1}{\partial x} & \dfrac{\partial v_1}{\partial y} + \varepsilon^2 \dfrac{\partial v_2}{\partial x} \\ \dfrac{\partial v_1}{\partial y} + \varepsilon^2 \dfrac{\partial v_2}{\partial x} & 2\varepsilon\dfrac{\partial v_2}{\partial y} \end{pmatrix},$$

The momentum equations are

$$\begin{aligned} &\frac{\mathsf{Re}}{\varepsilon}\left(\frac{\partial v_1}{\partial t} + \frac{\partial v_1}{\partial x}v_1 + \frac{\partial v_1}{\partial y}v_2\right) \\ &\quad = -\frac{1}{\varepsilon^2}\frac{\partial P}{\partial x} + 2\frac{\partial}{\partial x}\left[\left(1 + \frac{\mathsf{Bn}}{2II_{\mathbf{D}}}\right)\frac{\partial v_1}{\partial x}\right] \end{aligned}$$

$$+\frac{1}{\varepsilon^2}\frac{\partial}{\partial y}\left[\left(1+\frac{\mathsf{Bn}}{2II_{\mathbf{D}}}\right)\left(\frac{\partial v_1}{\partial y}\ \ \varepsilon^2\frac{\partial v_2}{\partial x}\right)\right], \tag{28}$$

$$\frac{\mathsf{Re}}{\varepsilon}\left(\frac{\partial v_2}{\partial t}+\frac{\partial v_2}{\partial x}v_1+\frac{\partial v_2}{\partial y}v_2\right)=-\frac{1}{\varepsilon^4}\frac{\partial P}{\partial y}$$
$$+\frac{1}{\varepsilon^2}\left\{\frac{\partial}{\partial x}\left[\left(1+\frac{\mathsf{Bn}}{2II_{\mathbf{D}}}\right)\left(\frac{\partial v_1}{\partial y}\ +\ \varepsilon^2\frac{\partial v_2}{\partial x}\right)\right]+2\frac{\partial}{\partial y}\left[\left(1+\frac{\mathsf{Bn}}{2II_{\mathbf{D}}}\right)\frac{\partial v_2}{\partial y}\right]\right\}. \tag{29}$$

The model is consistent if $II_{\mathbf{S}} < \mathsf{Bn}$ for $y \in [0, \sigma]$, i.e.

$$\sqrt{\left(\frac{\partial f_1}{\partial y}+\varepsilon^2\frac{\partial f_2}{\partial x}\right)^2+2\varepsilon^2\left[\left(\frac{\partial f_1}{\partial x}\right)^2+\left(\frac{\partial f_2}{\partial y}\right)^2\right]}\leq\frac{\mathsf{Bn}\lambda^2\varepsilon}{\mathsf{Re}}. \tag{30}$$

and if $II_{\mathbf{S}} \geq \mathsf{Bn}$ for $y \in [\sigma, 1]$, i.e. $II_{\mathbf{D}} \geq 0$. Finally we notice that

$$\varepsilon[\![\, S_{12}\,]\!]=\varepsilon\left[\left(1+\frac{\mathsf{Bn}}{2II_{\mathbf{D}}}\right)\left(\frac{\partial v_1}{\partial y}+\varepsilon^2\frac{\partial v_2}{\partial x}\right)\right]_{y=\sigma^+}$$
$$-\frac{\mathsf{Re}}{\lambda^2}\left[\frac{\partial f_1}{\partial y}+\varepsilon^2\frac{\partial f_2}{\partial x}\right]_{y=\sigma^-}. \tag{31}$$

4.3.3 Asymptotic Expansion

The assumption $\varepsilon \ll 1$, allows to seek the unknown fields (i.e. v_1, v_2, P, etc.) in the following form

$$\phi=\sum_{j=0}^{\infty}\phi^{(j)}\varepsilon^j$$

Substituting into the governing equations we get a hierarchy of problems that must be matched together. The matching procedure requires the specification of Re, Bi, and λ^2. We consider: $\mathsf{Re} \leq \mathscr{O}(1)$, i.e. laminar flow and $\mathsf{Bn} = \mathscr{O}(1)$. We introduce the dimensionless parameter

$$\Gamma=\frac{\eta H}{\mu U}=\frac{\mathsf{Re}}{\lambda^2}, \tag{32}$$

and consider two different cases which correspond to different behaviors of the inner core:

(1) $\Gamma = \mathcal{O}(1)$.
(2) $\Gamma = \mathcal{O}(\varepsilon)$.

When $\Gamma = \mathcal{O}(1)$, namely $\mathsf{Re} = \mathcal{O}\left(\lambda^2\right)$, we have an almost rigid inner core, while the case $\Gamma = \mathcal{O}(\varepsilon)$, i.e. $\mathsf{Re} = \mathcal{O}\left(\varepsilon\lambda^2\right)$, corresponds to a " soft" inner core where deformations are non-negligible. Let us show that the first case leads to the classical Bingham model. Indeed, considering $\mathsf{Re} = \mathcal{O}\left(\lambda^2\right)$

$$\mathcal{O}(1) = \Gamma = \varepsilon\frac{t_c\eta}{\mu}, \quad \Rightarrow \quad \frac{t_c\eta}{\mu} = \mathcal{O}\left(\varepsilon^{-1}\right). \tag{33}$$

Evaluating the order of magnitude of the elastic stress S_{el} and of the viscous stress S_{vis} we have

$$S_{vis} = \mu\frac{U}{H} \qquad S_{el} = \delta\eta\frac{L}{H},$$

where δ is the dimensionless order of magnitude of the longitudinal displacement. The continuity of the shear stress at the interface yields

$$\frac{S_{el}}{S_{vis}} = \mathcal{O}(1) \qquad \Rightarrow \qquad \delta\frac{t_c\eta}{\mu} = \mathcal{O}(1). \tag{34}$$

Hence we find $\delta = \mathcal{O}(\varepsilon)$, meaning an almost uniform longitudinal displacement as in the classical Bingham model. In the second case

$$\mathsf{Re} = \mathcal{O}(\varepsilon\lambda^2) \qquad \Rightarrow \qquad \frac{t_c\eta}{\mu} = \mathcal{O}(1)$$

which entails $\delta = \mathcal{O}(1)$. As a consequence the longitudinal displacement is not uniform.

4.3.4 First Case: $\Gamma = \mathcal{O}(1)$

We start considering the elastic domain, and we focus on the zero order terms. From (27) we obtain $P^{(0)} = P^{(0)}(x, t)$. Next, since $[\![P]\!] = 0$ on the interface, we have that in the whole elastic region $P^{(0)} = P^{(0)}\left(x, \sigma^+, t\right)$. From (26) we have

$$\begin{cases} \dfrac{\partial^2 f_1{}^{(0)}}{\partial y^2} = 0, \\ \dfrac{\partial f_1{}^{(0)}}{\partial y}\Big|_{y=0} = 0, \end{cases} \quad \Longrightarrow \; f_1{}^{(0)} = f_1{}^{(0)}(x, t).$$

Mass conservation in the elastic domain becomes

$$\frac{\partial^2 f_1^{(0)}}{\partial x \partial t} + \frac{\partial^2 f_2^{(0)}}{\partial y \partial t} = 0. \tag{35}$$

Recalling (24) it is easy to show that

$$\frac{\partial}{\partial x}\left(\frac{\partial f_1^{(0)}}{\partial t}\right) = 0. \tag{36}$$

Therefore setting

$$\kappa = \frac{\partial f_1^{(0)}}{\partial t},$$

we have $\kappa = \kappa(t)$. From (21) we find

$$\kappa = v_1^{(0)}\left(x, \sigma^+, t\right). \tag{37}$$

From (35)

$$\frac{\partial f_2^{(0)}}{\partial t} \text{ depends only on } t.$$

and the transversal velocity vanishes everywhere in the elastic region, so that

$$v_2^{(0)}\left(x, \sigma^+, t\right) = 0. \tag{38}$$

Let us now consider relation (31) at the zero order approximation. We get

$$\frac{\mathsf{Re}}{\lambda^2}\left.\frac{\partial f_1^{(1)}}{\partial y}\right|_{y=\sigma^-} = \left[\left(1 + \frac{\mathsf{Bn}}{2II_{\mathbf{D}}^{(0)}}\right)\frac{\partial v_1^{(0)}}{\partial y}\right]_{y=\sigma^+}. \tag{39}$$

The latter forces to analyze the first order term in (26), (27), namely

$$\begin{cases} \dfrac{\partial^2 f_1^{(1)}}{\partial y^2} = \dfrac{\lambda^2}{\mathsf{Re}}\dfrac{\partial P^{(0)}}{\partial x}, \\ \left.\dfrac{\partial f_1^{(1)}}{\partial y}\right|_{y=0} = 0, \end{cases} \quad \Longrightarrow \quad f_1^{(1)} = \frac{\lambda^2}{2\,\mathsf{Re}}\frac{\partial P^{(0)}}{\partial x}y^2 + B(x,t).$$

Hence (39) becomes

$$\frac{\partial P^{(0)}}{\partial x}\sigma = \left[\left(1 + \frac{\mathsf{Bn}}{2II_{\mathbf{D}}^{(0)}}\right)\frac{\partial v_1^{(0)}}{\partial y}\right]_{y=\sigma^+}. \tag{40}$$

It is easy to show that

$$II_{\mathbf{S}} = \left|\frac{\partial P^{(0)}}{\partial x}\right| y + \mathscr{O}(\varepsilon)$$

in the elastic region so that condition (30) is fulfilled when

$$\left|\frac{\partial P^{(0)}}{\partial x}\right| \sigma \leq \mathsf{Bn}. \tag{41}$$

We now focus on the viscous part $\sigma < y < 1$. Here (29) entails $P^{(0)} = P^{(0)}(x, t)$, so that the pressure is uniform on any channel section. Next, we observe that

$$II_{\mathbf{S}} = \left|\frac{\partial v_1^{(0)}}{\partial y} + \mathsf{Bi}\ \mathrm{sign}\left(\frac{\partial v_1^{(0)}}{\partial y}\right)\right| + \mathscr{O}(\varepsilon)$$

and (39) can be rewritten as

$$\underbrace{\left|\frac{\partial P^{(0)}}{\partial x}\right|\sigma}_{II_{\mathbf{S}} \leq \mathsf{Bn}} = \underbrace{\left|\left.\frac{\partial v_1^{(0)}}{\partial y}\right|_{y=\sigma^+} + \mathsf{Bi}\ \mathrm{sign}\left(\left.\frac{\partial v_1^{(0)}}{\partial y}\right|_{y=\sigma^+}\right)\right|}_{II_{\mathbf{S}} \geq \mathsf{Bn}}.$$

We conclude that

$$\left.\frac{\partial v_1^{(0)}}{\partial y}\right|_{y=\sigma^+} = 0 \qquad \frac{\partial P^{(0)}}{\partial x}\sigma = \mathsf{Bi}\ \mathrm{sign}\left(\left.\frac{\partial v_1^{(0)}}{\partial y}\right|_{y=\sigma^+}\right). \tag{42}$$

Focussing now on (28) we find

$$-\frac{\partial P^{(0)}}{\partial x} + \frac{\partial}{\partial y}\left[\frac{\partial v_1^{(0)}}{\partial y} + \mathsf{Bi}\ \mathrm{sign}\left(\frac{\partial v_1^{(0)}}{\partial y}\right)\right] = 0,$$

so that

$$\begin{cases} -\dfrac{\partial P^{(0)}}{\partial x} + \dfrac{\partial^2 v_1^{(0)}}{\partial y^2} = 0, \\ v_1^{(0)}(x, h, t) = 0, \\ \left.\dfrac{\partial v_1^{(0)}}{\partial y}\right|_{y=\sigma^+} = 0, \end{cases} \tag{43}$$

Solving (43) we get

$$v_1^{(0)}(x, y, t) = -\frac{1}{2}\frac{\partial P^{(0)}}{\partial x}\left(h^2 - y^2\right) + \mathsf{Bi}\,\mathrm{sign}\left(\left.\frac{\partial v_1^{(0)}}{\partial y}\right|_{y=\sigma^+}\right)(h - y). \tag{44}$$

In particular, (37) yields

$$\kappa = -\frac{1}{2}\frac{\partial P^{(0)}}{\partial x}(h - \sigma)^2, \quad \text{with} \quad \omega = \omega(t). \tag{45}$$

Remark 2 We remark that

$$\kappa = -\frac{\mathsf{Bn}}{2\sigma}\mathrm{sign}\left(\left.\frac{\partial v_1^{(0)}}{\partial y}\right|_{y=\sigma^+}\right)(h - \sigma)^2. \tag{46}$$

Therefore the derivative w.r.t. x of the r.h.s. of (46) must vanish and

$$\frac{\partial h}{\partial x} = \frac{h + \sigma}{2\sigma}\frac{\partial \sigma}{\partial x}. \tag{47}$$

From (18)

$$\int_\sigma^h \frac{\partial v_1^{(0)}}{\partial x} dy = 0, \tag{48}$$

since $v_2^{(0)}(x, h, t) = v_2^{(0)}\left(x, \sigma^+, t\right) = 0$. Hence, exploiting (44)

$$\frac{\partial v_1^{(0)}}{\partial x} = -\frac{1}{2}\frac{\partial^2 P^{(0)}}{\partial x^2}\left(h^2 - y^2\right) - \frac{\partial P^{(0)}}{\partial x}\frac{\partial h}{\partial x}h + \frac{\partial P^{(0)}}{\partial x}\sigma\frac{\partial h}{\partial x}.$$

Thus (48) yields

$$(h-\sigma)^2\left[\frac{1}{6}\frac{\partial^2 P^{(0)}}{\partial x^2}(\sigma+2h)+\frac{\partial P^{(0)}}{\partial x}\frac{\partial h}{\partial x}\right]=0. \tag{49}$$

In case h is uniform we get

$$\frac{\partial^2 P^{(0)}}{\partial x^2}=0 \quad \Rightarrow \quad P^{(0)}(x,t)=P_{in}(t)-x\Delta P(t),$$

and

$$\sigma(t)=\frac{\mathsf{Bn}}{\Delta P(t)},$$

from which we derive the classical Bingham flow condition we find in [4]

$$\frac{\mathsf{Bn}}{\Delta P(t)}<h,$$

ensuring the flow within the channel.

Remark 3 In case h does depend on x (49) does not give rise to any solution consistent with (47) (a well known paradox of the Bingham model). Indeed, form $(42)_2$

$$\frac{\partial^2 P^{(0)}}{\partial x^2}=-\frac{1}{\sigma}\frac{\partial \sigma}{\partial x}\frac{\partial P^{(0)}}{\partial x},$$

that inserted into (49) yields

$$\frac{\partial P^{(0)}}{\partial x}(h-\sigma)^2\left[\frac{\partial h}{\partial x}-\frac{\partial \sigma}{\partial x}\frac{\sigma+2h}{6\sigma}\right]=0.$$

The above implies

$$\frac{\partial \sigma}{\partial x}\frac{\sigma+2h}{6\sigma}=\frac{\partial h}{\partial x} \tag{50}$$

Inserting (50) into (47) we get $h=-2\sigma$, that is a contradiction (lubrication paradox, see [6, 17, 21, 27]).

4.3.5 Second Case $\Gamma = \mathscr{O}(\varepsilon)$

Set $\varepsilon\hat{\Gamma} = \Gamma$ with $\hat{\Gamma} = \mathscr{O}(1)$. From (31)

$$\left[\left(1+\frac{\mathsf{Bn}}{2II_{\mathbf{D}}}\right)\left(\frac{\partial v_1}{\partial y}+\varepsilon^2\frac{\partial v_2}{\partial x}\right)\right]_{y=\sigma^+} = \hat{\Gamma}\left[\frac{\partial f_1}{\partial y}+\varepsilon^2\frac{\partial f_2}{\partial x}\right]_{y=\sigma^-}, \tag{51}$$

Once again $P^{(0)} = P^{(0)}(x,t)$ in the whole domain. In the elastic part

$$\begin{cases} \dfrac{\partial^2 f_1^{(0)}}{\partial y^2} = \dfrac{1}{\hat{\Gamma}}\dfrac{\partial P^{(0)}}{\partial x}, \\ \left.\dfrac{\partial f_1^{(0)}}{\partial y}\right|_{y=0} = 0, \end{cases} \quad \Rightarrow \quad f_1^{(0)} = \frac{1}{2\hat{\Gamma}}\frac{\partial P^{(0)}}{\partial x}y^2 + a(x,t), \tag{52}$$

so that (51) implies

$$\frac{\partial P^{(0)}}{\partial x}\sigma = \left[\left(1+\frac{\mathsf{Bn}}{2II_{\mathbf{D}}^{(0)}}\right)\frac{\partial v_1^{(0)}}{\partial y}\right]_{y=\sigma^+}.$$

The term $a(x,t)$ is unknown at this stage while $v_1^{(0)}$ is

$$v_1^{(0)} = \frac{1}{2\hat{\Gamma}}\frac{\partial^2 P^{(0)}}{\partial t \partial x}y^2 + \kappa(x,t),$$

where now

$$\kappa(x,t) = \frac{\partial a(x,t)}{\partial t}, \tag{53}$$

can be interpreted as the uniform part of the longitudinal velocity. Checking condition (30) we find again (41).

Remark 4 At the leading order the longitudinal displacement is a superposition of a uniform displacement $a(x,t)$ and a non uniform displacement modulated by the pressure gradient. The latter becomes negligible for large values of $\hat{\Gamma}$ and the first case is recovered for $\hat{\Gamma} \gg 1$.

In the fluid region

$$\frac{\partial P^{(0)}}{\partial x}\sigma = -\mathsf{Bn}.$$

Moreover

$$v_1^{(0)}(x,y,t) = -\frac{1}{2}\frac{\partial P^{(0)}}{\partial x}\left(h^2 - y^2\right) + \frac{\partial P^{(0)}}{\partial x}\sigma\,(h-y)\,.$$

The jump condition (21) yields

$$\frac{1}{2\,\hat{\Gamma}}\frac{\partial^2 P^{(0)}}{\partial t \partial x}\sigma^2 + \omega\,(x,t) = -\frac{1}{2}\frac{\partial P^{(0)}}{\partial x}\,(h-\sigma)^2\,,$$

with ω given by (53). From mass balance and boundary conditions

$$0 = \int_0^h \frac{\partial v_1^{(0)}}{\partial x}dy = \int_0^\sigma \frac{\partial}{\partial x}\left(\frac{\partial f_1^{(0)}}{\partial t}\right)dy + \int_\sigma^h \frac{\partial v_1^{(0)}}{\partial x}dy,$$

which, after some of algebra, gives

$$(h-\sigma)^2\left[\frac{1}{6}\frac{\partial^2 P^{(0)}}{\partial x^2}\,(2h+\sigma) + \frac{\partial P^{(0)}}{\partial x}\frac{\partial h}{\partial x}\right] - \frac{\sigma^3}{6\,\hat{\Gamma}}\frac{\partial^3 P^{(0)}}{\partial x^2 \partial t} - \sigma\frac{\partial \omega}{\partial x} = 0.$$

Therefore the mathematical problem at the zero order approximation is the following

$$\begin{cases} \dfrac{\partial P^{(0)}}{\partial x}\sigma = -\mathsf{Bn}, \\[2ex] \dfrac{1}{2\,\hat{\Gamma}}\dfrac{\partial^2 P^{(0)}}{\partial t \partial x}\sigma^2 + \kappa\,(x,t) = -\dfrac{1}{2}\dfrac{\partial P^{(0)}}{\partial x}\,(h-\sigma)^2\,, \\[2ex] -(h-\sigma)^2\left[\dfrac{1}{6}\dfrac{\partial^2 P^{(0)}}{\partial x^2}\,(2h+\sigma) + \dfrac{\partial P^{(0)}}{\partial x}\dfrac{\partial h}{\partial x}\right] \\ \qquad + \dfrac{\sigma^3}{6\,\hat{\Gamma}}\dfrac{\partial}{\partial t}\left(\dfrac{\partial^2 P^{(0)}}{\partial x^2}\right) + \sigma\dfrac{\partial \kappa}{\partial x} = 0. \end{cases} \tag{54}$$

Example 1 Consider the stationary problem when $h \equiv 1$

$$\begin{cases} \dfrac{\partial P^{(0)}}{\partial x}\sigma = -\mathsf{Bn}, \;\Rightarrow\; \dfrac{\partial \sigma}{\partial x}\dfrac{\partial P^{(0)}}{\partial x} = -\dfrac{\partial^2 P^{(0)}}{\partial x^2}\sigma, \\[2ex] \kappa\,(x,t) = -\dfrac{1}{2}\dfrac{\partial P^{(0)}}{\partial x}\,(1-\sigma)^2\,, \;\Rightarrow\; \dfrac{\partial \kappa}{\partial x} = -\dfrac{1}{2}\dfrac{\partial^2 P^{(0)}}{\partial x^2}\left(1-\sigma^2\right), \\[2ex] -\dfrac{(1-\sigma)^2}{6}\dfrac{\partial^2 P^{(0)}}{\partial x^2}\,(2+\sigma) + \sigma\dfrac{\partial \kappa}{\partial x} = 0. \end{cases} \tag{55}$$

We get

$$\frac{1}{3}\frac{\partial^2 P^{(0)}}{\partial x^2}\left(1-\sigma^3\right)=0,$$

yielding $\sigma = 1$ (which we do not consider) and $P^{(0)} = P_{in} - \Delta P x$, with ΔP known. Therefore

$$\sigma = = \frac{\mathsf{Bn}}{\Delta P}, \tag{56}$$

$$\kappa = \frac{\Delta P}{2}\left(1-\frac{\mathsf{Bn}}{\Delta P}\right)^2. \tag{57}$$

Requiring $\sigma < 1$ we get the usual Bingham flow condition.

4.3.6 Stationary Version of (54)

We show that the stationary version of system (54), namely

$$\begin{cases} \dfrac{\partial P^{(0)}}{\partial x}\sigma = -\mathsf{Bn}, \\ \omega(x,t) = -\dfrac{1}{2}\dfrac{\partial P^{(0)}}{\partial x}(h-\sigma)^2, \\ -(h-\sigma)^2\left[\dfrac{1}{6}\dfrac{\partial^2 P^{(0)}}{\partial x^2}(2h+\sigma)+\dfrac{\partial P^{(0)}}{\partial x}\dfrac{\partial h}{\partial x}\right]+\sigma\dfrac{\partial \omega}{\partial x}=0, \end{cases} \tag{58}$$

admits a unique solution when h is a smooth bounded function of x with $h \in [h_m, h_M]$. From $(58)_1$

$$\frac{\partial^2 P^{(0)}}{\partial x^2} = \frac{\mathsf{Bn}}{\sigma^2}\frac{\partial \sigma}{\partial x}, \tag{59}$$

and from $(58)_2$

$$\kappa(x,t) = \frac{\mathsf{Bn}}{2\,\sigma}(h-\sigma)^2, \quad \text{and} \quad \frac{\partial \kappa}{\partial x} = \frac{\mathsf{Bn}\ (h-\sigma)}{2\sigma^2}\left[2\sigma\frac{\partial h}{\partial x}-\frac{\partial \sigma}{\partial x}(h+\sigma)\right].$$

Hence, system (58) can be rewritten as

$$\begin{cases} \dfrac{\partial P^{(0)}}{\partial x}\sigma = -\mathsf{Bn}, \\ \\ -(h-\sigma)^2\left[\dfrac{1}{6}\dfrac{\partial^2 P^{(0)}}{\partial x^2}(2h+\sigma) + \dfrac{\partial P^{(0)}}{\partial x}\dfrac{\partial h}{\partial x}\right] + \\ \dfrac{\mathsf{Bn}\ (h-\sigma)}{2\sigma}\left[2\sigma\dfrac{\partial h}{\partial x} - \dfrac{\partial \sigma}{\partial x}(h+\sigma)\right] = 0. \end{cases} \tag{60}$$

In [10] it has been proved that there exists a unique pair of sufficiently regular functions $\left(\sigma(x), P^{(0)}(x)\right)$ such that:

(a) $0 < \sigma(x) < h(x)$, for all $x \in [0, 1]$.
(b) $P^{(0)}(0) = P_{in}$, and $P^{(0)}(1) = P_{in} - \Delta P$.
(c) $\sigma(x)$ and $P^{(0)}(x)$ fulfill the equations of (60).

Remark 5 Assuming that (60) is solvable according to the above definition, we find immediately a new "flow condition". Indeed, integrating $(60)_1$ between 0 and 1, we obtain

$$\frac{\Delta P}{\mathsf{Bn}} = \int_0^1 \frac{dx}{\sigma(x)}.$$

Since

$$\int_0^1 \frac{dx}{\sigma(x)} > \int_0^1 \frac{dx}{h(x)}, \tag{61}$$

if (60) admits a solution, the following inequality holds true

$$\frac{\Delta P}{\mathsf{Bn}} > \int_0^1 \frac{dx}{h(x)}. \tag{62}$$

Going back to dimension variables we get

$$\frac{\Delta P}{\tau_o} > \int_0^L \frac{dx}{H(x)},$$

which generalizes the classical Bingham flow condition.

4.4 Numerical Simulations

We present some numerical simulations to investigate the stationary behavior of $\sigma(x)$ when $\Gamma = \mathcal{O}(1)$. Suppose following function

$$h(x) = \frac{1}{2} - \frac{1}{10}\arctan\left[200\left(x - \frac{1}{2}\right)\right],$$

The channel profile and the free boundary separating the elastic and the viscous phase are shown in Figs. 11, 12, 13, 14 for different values of $\Delta P/\mathsf{Bn}$ satisfying condition (62). We see that

$$\int_0^1 \frac{dx'}{h(x')} = 2.2,$$

and consequently we perform numerical simulation with $\Delta P/\mathsf{Bn} > 2.2$.
The amplitude of the inner core decreases as $\Delta P/\mathsf{Bn}$ increases. When $\Delta P/\mathsf{Bn} \gg 1$ (Fig. 14), the inner core approximately disappears and the system becomes almost purely viscous. In the same way, we observe that when $\Delta P/\mathsf{Bn}$ is close to 2.2 then $\sigma \to h$ (Fig. 11) and the viscous part tends to disappear. Also in this case we speak of a limit, since condition (62) must be fulfilled.

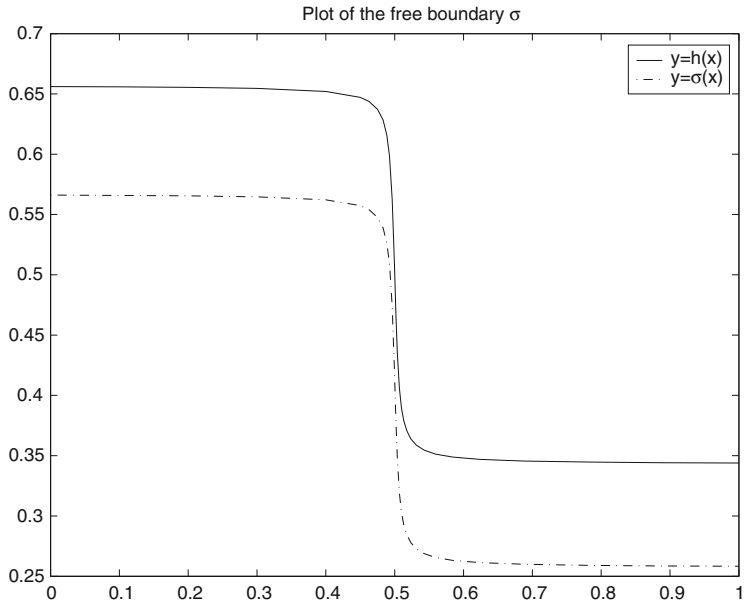

Fig. 11 Plot of the free boundary (dashed line) $y = \sigma(x)$ with $\Delta P/\mathsf{Bn} = 2.5$ and with condition (62) fulfilled

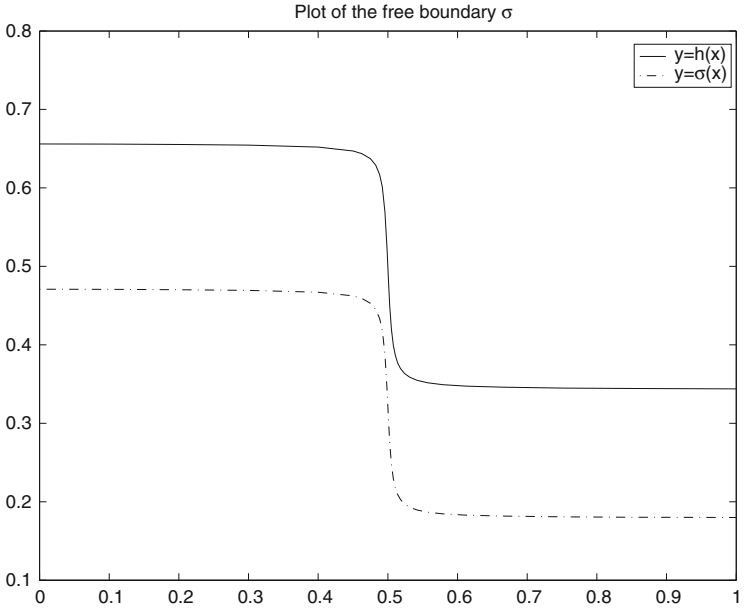

Fig. 12 Plot of the free boundary (dashed line) $y = \sigma(x)$ with $\Delta P/\mathsf{Bn} = 3.5$ and with condition (62) fulfilled

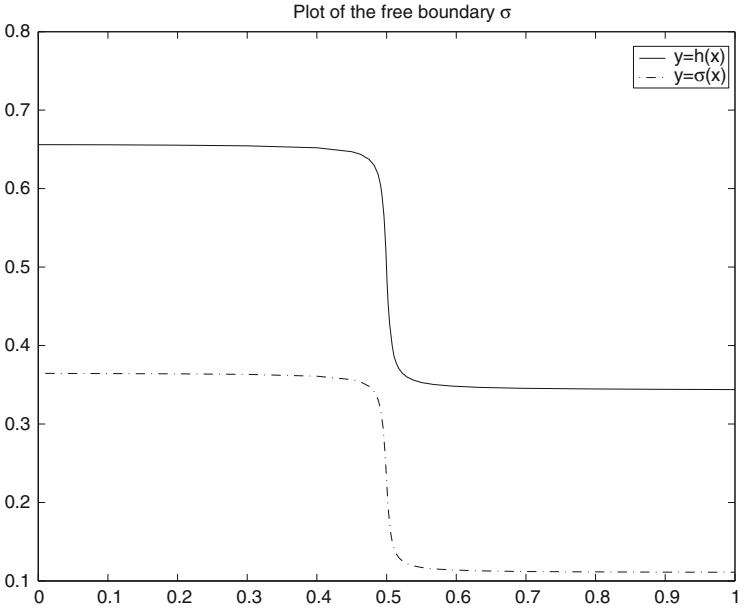

Fig. 13 Plot of the free boundary (dashed line) $y = \sigma(x)$ with $\Delta P/\mathsf{Bn} = 5.5$ and with condition (62) fulfilled

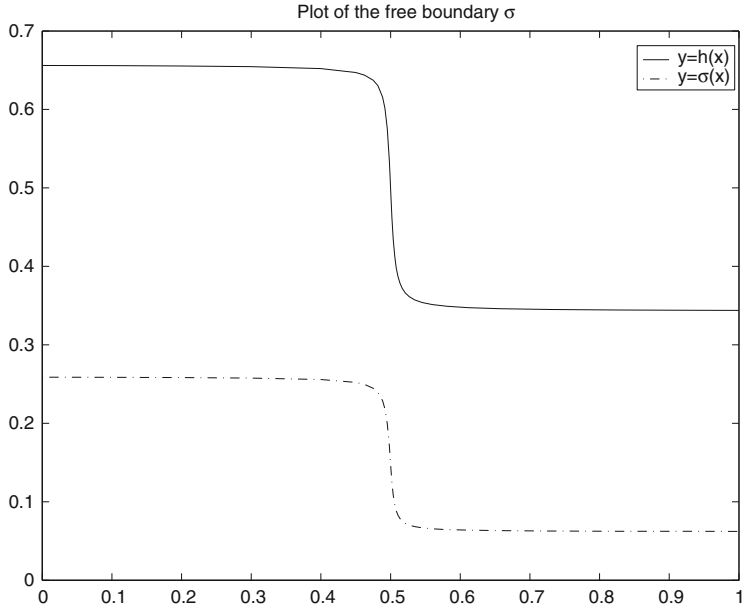

Fig. 14 Plot of the free boundary (dashed line) $y = \sigma(x)$ with $\Delta P/\mathsf{Bn} = 9.5$ and with condition (62) fulfilled

5 Two Dimensional Channel Flow: A New Approach

To model the flow of a Bingham fluid one considers the balance of linear momentum written in the differential form

$$\rho \frac{D\mathbf{v}}{Dt} = -\nabla P + \nabla \cdot \mathbf{S}, \tag{63}$$

where ρ is density, $\mathbf{v}$ is velocity, P is pressure and $\mathbf{S}$ is the deviatoric part of the stress. Equation (63) is typically used in the whole domain, assuming that the velocity and the stress are continuous across the fluid/rigid interface. Within the liquid domain the fluid is assumed to behave as a viscous incompressible fluid, whereas in the rigid part the stress is indetermined. Indeed in the unyielded part we only know that the strain rate vanishes, i.e. $\mathbf{D} = 0$. Assuming that Eq. (63) holds in every part of the domain may lead to paradoxes, as the one that occurs in lubrication regimes, [6, 17].

To avoid this occurrence we propose a novel approach which essentially consists in using a integral formulation for the balance of linear momentum within the unyielded part. We apply this approach to study the flow in a bidimensional channel

of varying amplitude, with the driving force being an applied pressure gradient (Poiseuille flow). We assume that the aspect ratio of the channel is small, so that the lubrication approximation is suitable. In this case, Eq. (63) can be simplified introducing the ratio $\varepsilon \ll 1$ between the length and the maximum amplitude and rescaling the problem in a nondimensional form. The solution can be sought as power series of ε, where the leading order is the one we are interested in. With this procedure one tacitly assumes that the nondimensional variables and their derivatives are $\mathcal{O}(1)$ in the liquid and solid domain. In particular the stress components S_{ij} are assumed to be everywhere $\mathcal{O}(1)$, but this latter hypothesis can be checked "a posteriori" only in the liquid part, since in the rigid domain the stress is not determined.

This point is the central importance for our procedure. Indeed, the assumption $S_{ij} = \mathcal{O}(1)$ and the use of (63) to derive the motion in the rigid part, leads to the well known "lubrication paradox" , which consists in a plug velocity that depends on the longitudinal coordinate. Note that the paradox disappears when one considers a deformable core, as shown in the previous sections. If one does not use Eq. (63) in the unyielded part and write the balance of linear momentum using an integral global approach similar to the one presented in [29] and in [28], the paradox is no longer present. Therefore, the unyielded part is treated as an evolving non material volume Ω_t and its dynamics is modelled writing the balance of linear momentum as

$$\int_{\Omega_t} \frac{\partial}{\partial t} (\rho \mathbf{v})\, dV + \int_{\partial \Omega_t} \rho \mathbf{v}\, (\mathbf{v} \cdot \mathbf{n})\, dS = \int_{\partial \Omega_t} (\mathbf{T}\mathbf{n}) dS, \tag{64}$$

where $\mathbf{T} = -P\mathbf{I} + \mathbf{S}$, is the Cauchy stress tensor and $\mathbf{w}$ the velocity of the boundary $\partial \Omega_t$. The advantage of this approach lies in the fact that the knowledge of the stress inside the rigid part is no longer needed and no guess has to be made on the order of magnitude of the stress components. Only the stress acting on the boundary of Ω_t is required.

Therefore we need to know: (1) the forces acting on the yield surface σ (see Fig. 15); (2) the forces acting on the inlet and outlet of the channel. On σ the viscous stress is given once the problem in the viscous domain is solved. On the channel inlet and outlet the applied pressure, assumed to be a given datum of the problem, is required.

When dealing with the leading order approximation in the channel flow, Eq. (64) becomes an integro-differential equation for the pressure P, whose solution allows to determine explicit expressions for the velocity field $\mathbf{v}$ and the yield surface σ. We prove that the longitudinal velocity is spatially uniform, while the transversal velocity vanishes (no paradox). We also show that these results can be also extended to the case of fluids with constant density and pressure dependent viscosity.

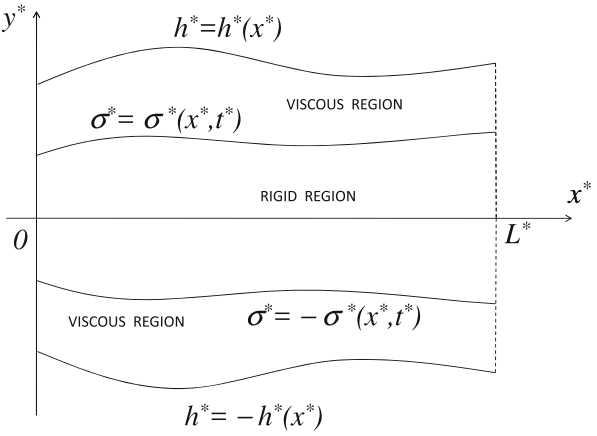

Fig. 15 Sketch of the domain of the problem

5.1 The Physical Model

Let us consider the flow of an incompressible Bingham fluid in a channel of length L and amplitude $2h\,(x)$. Because of symmetry, we may limit our analysis to the upper part of the layer $[0, h(x)]$. The velocity field is given by

$$\mathbf{v} = v_1(x, y, t)\mathbf{i} + v_2(x, y, t)\mathbf{j},$$

The Cauchy stress is $\mathbf{T} = -P\mathbf{I}+\mathbf{S}$, where the deviatoric part is the one of a Bingham fluid

$$\mathbf{S} = \left(2\mu + \frac{\tau_o}{II_{\mathbf{D}}}\right)\mathbf{D}. \tag{65}$$

In the above μ is the viscosity, τ_o is the yield stress. If $\mathbf{D} \neq 0$ we get

$$II_{\mathbf{S}} = 2\mu II_{\mathbf{D}} + \tau_o$$

which holds with $II_{\mathbf{S}} \geq \tau_o$. Therefore, whenever $\mathbf{D} = 0$, we have $II_{\mathbf{S}} \leq \tau_o$ and the stress is not determined. We assume that the viscous and the rigid regions are separated by a sharp interface $y = \pm\sigma\,(x, t)$. Assuming incompressibility we write

$$\text{tr}\,\mathbf{D} = \frac{\partial v_1}{\partial x} + \frac{\partial v_2}{\partial y} = 0. \tag{66}$$

5.2 The Viscous Domain

We write the governing equations in the viscous region neglecting body forces. These are the incompressibility condition (66) and

$$\rho\left(\frac{\partial v_1}{\partial t}+v_1\frac{\partial v_1}{\partial x}+v_2\frac{\partial v_1}{\partial y}\right)=-\frac{\partial P}{\partial x}+\frac{\partial S_{11}}{\partial x}+\frac{\partial S_{12}}{\partial y}, \tag{67}$$

$$\rho\left(\frac{\partial v_2}{\partial t}+v_1\frac{\partial v_2}{\partial x}+v_2\frac{\partial v_2^*}{\partial y}\right)=-\frac{\partial P}{\partial y}+\frac{\partial S_{12}}{\partial x}+\frac{\partial S_{22}}{\partial y}, \tag{68}$$

5.3 The Rigid Domain

The rigid domain Ω_t at some time $t>0$ is given by

$$\Omega_t=\{(x,y):\quad x\in[0,L],\quad y\in[-\sigma,\sigma]\}.$$

The integral momentum balance for the whole domain Ω_t in the absence of body forces is given by (64). Focussing on the upper part of the domain ($y>0$) we find that (64) can be rewritten as

$$2\frac{\partial}{\partial t}(\rho\mathbf{v})\int_0^L\sigma(x,t)dx+2\rho\mathbf{v}\int_0^L\frac{\partial\sigma}{\partial t}(x,t)dx=\int_{\partial\Omega_t}\mathbf{Tn}\,dS.$$

The external forces acting on the boundary $\partial\Omega_t$ are expressed by the surface integral on the r.h.s. Assuming that P_{in}, P_{out} are the (uniform) pressures acting on the inlet and outlet of the channel, we find

$$\begin{aligned}\int_{\partial\Omega_t}(\mathbf{Tn})dS=2\int_0^L\begin{bmatrix}(-\sigma_xT_{11}+T_{12})_\sigma\\ \\ 0\end{bmatrix}dx\\ +2\int_0^{\sigma_{out}}\begin{pmatrix}-P_{out}\\ \\ 0\end{pmatrix}dy+2\int_0^{\sigma_{in}}\begin{pmatrix}P_{in}\\ \\ 0\end{pmatrix}dy,\end{aligned}$$

where $\sigma_{in}=\sigma(0,t)$, $\sigma_{out}=\sigma(L,t)$. Recalling that in the rigid plug velocity is

$$\begin{cases}v_1=k_1(t),\\ \\ v_2=k_2(t)=0\quad(\text{by symmetry}),\end{cases} \tag{69}$$

the dynamics of the whole rigid region is expressed only by the first component of (64), that is

$$\int_0^L \frac{\partial}{\partial t}\left(\rho k_1 \sigma\right) dx = \int_0^L \left[-\sigma_x T_{11} + T_{12}\right]_\sigma \, dx + P_{in}\sigma_{in} - P_{out}\sigma_{out}, \tag{70}$$

Hence the prescribed pressure difference driving the flow is

$$\Delta P = P_{in} - P_{out}. \tag{71}$$

The boundary condition on the channel wall is

$$\mathbf{v}(x, h, t) = 0 \tag{72}$$

i.e. the no-slip condition. On σ we impose

$$\left[\!\left[\mathbf{v}\cdot\mathbf{t}\right]\!\right]_{y=\sigma} = 0, \qquad \left[\!\left[\mathbf{v}\cdot\mathbf{n}\right]\!\right]_{y=\sigma} = 0, \tag{73}$$

$$\left[\!\left[\mathbf{T}\mathbf{n}\cdot\mathbf{t}\right]\!\right]_{y=\sigma} = 0, \qquad \left[\!\left[\mathbf{T}\mathbf{n}\cdot\mathbf{n}\right]\!\right]_{y=\sigma} = 0, \tag{74}$$

which express the continuity of the velocity and of the stress across the yield surface $y = \sigma$ ($\mathbf{t}$ and $\mathbf{n}$ are the tangent and normal unit vector to σ).

Remark 6 In Sect. 5.10 we will extend our model the case in which the viscosity depends on pressure, namely $\mu = \mu\mu\,(P)$.

5.4 Scaling

Set

$$H = \sup_{x\in[0,L]} h(x),$$

and introduce

$$\varepsilon = \frac{H}{L} \ll 1,$$

which is crucial for applying the classical thin film approach. We rescale the problem using the following non dimensional variables

$$\tilde{x} = \frac{x}{L}, \qquad \tilde{y} = \frac{y}{\varepsilon L}, \qquad \tilde{\sigma} = \frac{\sigma}{\varepsilon L}, \qquad \tilde{h} = \frac{h}{\varepsilon L}, \qquad \tilde{t} = \frac{t}{(L/U)},$$

$$\tilde{v}_1 = \frac{v_1}{U}, \quad v_2 = \frac{v_2}{\varepsilon U}, \quad \tilde{P} = \frac{P - P_{out}}{P_c}, \quad \Delta\tilde{P} = \frac{\Delta P}{P_c}, \tag{75}$$

$$\tilde{\mathbf{S}} = \frac{\mathbf{S}}{(\mu U/H)}, \quad \tilde{\mathbf{D}} = \frac{\mathbf{D}}{(U/H)}, \quad \tilde{II}_D = \frac{II_D}{(U/H)}, \quad \tilde{II}_S = \frac{II_S}{(\mu U/H)},$$

where we select the reference pressure using the Poiseuille formula

$$P_c = \frac{\mu L U}{H^2} \tag{76}$$

After some algebra (and neglecting the tildas) we find

$$\mathbf{S} = \left(2 + \frac{\mathsf{Bn}}{II_D}\right)\mathbf{D},$$

where

$$\mathsf{Bn} = \frac{\tau_o H}{\mu U}$$

is the Bingham number. Moreover

$$II_D = \sqrt{\varepsilon^2\left(\frac{\partial v_1}{\partial x}\right)^2 + \frac{1}{4}\left(\frac{\partial v_1}{\partial y} + \varepsilon^2\frac{\partial v_2}{\partial x}\right)^2}.$$

Equations (66)–(68) become

$$\frac{\partial v_1}{\partial x} + \frac{\partial v_2}{\partial y} = 0, \tag{77}$$

$$\varepsilon\mathsf{Re}\left(\frac{\partial v_1}{\partial t} + v_1\frac{\partial v_1}{\partial x} + v_2\frac{\partial v_1}{\partial y}\right) = -\frac{\partial P}{\partial x} + \varepsilon\frac{\partial S_{11}}{\partial x} + \frac{\partial S_{12}}{\partial y}, \tag{78}$$

$$\varepsilon^3\mathsf{Re}\left(\frac{\partial v_2}{\partial t} + v_1\frac{\partial v_2}{\partial x} + v_2\frac{\partial v_2}{\partial y}\right) = -\frac{\partial P}{\partial y} + \varepsilon^2\frac{\partial S_{12}}{\partial x} + \varepsilon\frac{\partial S_{22}}{\partial y}, \tag{79}$$

where

$$\mathsf{Re} = \left(\frac{\rho U H}{\mu}\right)$$

is the Reynolds number. The inner core equation (70) becomes

$$\varepsilon\mathsf{Re}\int_0^1 \frac{\partial}{\partial t}(k_1\sigma)dx = \int_0^1 \left[P\sigma_x - \varepsilon\sigma_x S_{11} + S_{12}\right]_{\sigma^+} dx + \Delta P\sigma_{in}. \tag{80}$$

The boundary conditions (72)–(74) become

$$\mathbf{v}(x, h, t) = 0, \tag{81}$$

$$[\![v_1]\!]_{y=\sigma} = [\![v_2]\!]_{y=\sigma} = 0, \tag{82}$$

$$\begin{cases} [\![P]\!]\left[1 + \varepsilon^2\left(\dfrac{\partial\sigma}{\partial x}\right)^2\right]_{y=\sigma} + \left[\varepsilon^3 S_{11}\left(\dfrac{\partial\sigma}{\partial x}\right)^2 - 2\varepsilon^2 S_{12}\left(\dfrac{\partial\sigma}{\partial x}\right) + \varepsilon S_{22}\right]_{y=\sigma} = 0, \\ [\![S_{12}]\!]_{y=\sigma} + \varepsilon\left(\dfrac{\partial\sigma}{\partial x}\right)\left[S_{22} - S_{11} - \varepsilon S_{12}\dfrac{\partial\sigma}{\partial x}\right]_{y=\sigma} = 0. \end{cases} \tag{83}$$

In the rigid domain the non dimensional velocity field is

$$\begin{cases} v_1 = k_1(t), \\ v_2 = 0, \end{cases} \tag{84}$$

with $k_1 = k_1/U$.

5.5 The Leading Order Approximation

We look for a solution in which the main variables of the problem can be expressed as power series of ε

$$\mathbf{v} = \sum_{j=0}^{\infty} \mathbf{v}^{(j)}\varepsilon^j \qquad P = \sum_{j=0}^{\infty} P^{(j)}\varepsilon^j \qquad \sigma = \sum_{j=0}^{\infty} \sigma^{(j)}\varepsilon^j$$

We further assume that $h(x)$ is such that

$$\frac{\partial h}{\partial x} = O(1)$$

and we limit our analysis to the leading order, assuming that $\mathsf{Bi} = \mathscr{O}(1)$ and $\mathsf{Re} \leqslant \mathscr{O}(1)$. We begin by observing that

$$S_{12}^{(0)} = \left[1 + \frac{\mathsf{Bn}}{|v_{1y}^{(0)}|}\right] v_{1y}^{(0)},$$

and, since we are looking for a solution with $v_{1y}^{(0)} < 0$ in the upper part of the channel, we write

$$S_{12}^{(0)} = v_{1y}^{(0)} - \mathsf{Bn}.$$

The problem reduces to

$$\begin{cases} \dfrac{\partial v_1^{(0)}}{\partial x} + \dfrac{\partial v_2^{(0)}}{\partial y} = 0, \\ -\dfrac{\partial P^{(0)}}{\partial x} + \dfrac{\partial}{\partial y}\left(\dfrac{\partial v_1^{(0)}}{\partial y}\right) = 0, \\ -\dfrac{\partial P^{(0)}}{\partial y} = 0, \end{cases} \tag{85}$$

with boundary conditions

$$\begin{cases} \left.\dfrac{\partial v_1^{(0)}}{\partial y}\right|_{y=\sigma^{(0)}} = 0, \\ v_1^{(0)}(x,h,t) = 0. \end{cases} \tag{86}$$

Integrating we find

$$v_1^{(0)} = -P_x^{(0)} \frac{(h-y)(y-2\sigma^{(0)}+h)}{6}. \tag{87}$$

Exploiting the continuity equation we get

$$v_2^{(0)} = -\frac{\partial}{\partial x}\left[P_x^{(0)} \frac{(y-h)^2(y-3\sigma^{(0)}+2h)}{6}\right]. \tag{88}$$

Evaluating the velocity components on the yield surface we get

$$\left.v_1^{(0)}\right|_{y=\sigma^{(0)}} = k_1^{(0)}(t) = -P_x^{(0)} \frac{(h-\sigma^{(0)})^2}{2}, \tag{89}$$

$$\left.v_2^{(0)}\right|_{y=\sigma^{(0)}} = \frac{\partial}{\partial x}\left[-P_x^{(0)} \frac{(h-\sigma^{(0)})^3}{3}\right] - \sigma_x^{(0)} P_x^{(0)} \frac{(h-\sigma^{(0)})^2}{2} = 0,$$

which entails

$$\underbrace{\left(-P_x^{(0)}\frac{(h-\sigma^{(0)})^2}{2}\right)}_{k_1^{(0)}}\cdot\frac{\partial}{\partial x}\left[\frac{2}{3}(h-\sigma^{(0)})\right]=-\sigma_x^{(0)}\underbrace{\left(-P_x^{(0)}\frac{(h-\sigma^{(0)})^2}{2}\right)}_{k_1^{(0)}}.$$

Supposing $k_1^{(0)}\neq 0$, we find

$$\sigma^{(0)}(x,t)=-2h(x)-C, \tag{90}$$

where C is unknown. Let us now consider the rigid core equation (80) at the zero order

$$\int_0^1 P^{(0)}\sigma_x^{(0)}dx-\mathsf{Bn}+\Delta P\sigma_{in}^{(0)}=0,$$

which, after an integration by parts, reduces to

$$-\int_0^1 P_x^{(0)}\sigma^{(0)}dx=\mathsf{Bn}. \tag{91}$$

Substituting (90) into (91), we obtain

$$C=\frac{2\int_0^1 P_x^{(0)}hdx-\mathsf{Bn}}{\Delta P}.$$

We thus have

$$\sigma^{(0)}=-2h(x)+\frac{\mathsf{Bi}-2\int_0^1 P_x^{(0)}h\,dx}{\Delta P}, \tag{92}$$

or equivalently

$$\sigma^{(0)}=2(h_{in}-h(x))+\frac{\mathsf{Bi}}{\Delta P}+\frac{2}{\Delta P}\int_0^1 P^{(0)}h_x dx, \tag{93}$$

where $h_{in}=h(0)$. Defining the viscous region width as

$$\ell^{(0)}=h(x)-\sigma^{(0)}(x,t), \tag{94}$$

formula (92) entails

$$\ell^{(0)} = 3h\,(x) + \frac{2\int_0^1 P_x^{(0)} h\,dx - \mathsf{Bn}}{\Delta P}. \tag{95}$$

Hence

$$k_1^{(0)} = -P_x^{(0)} \frac{\ell^{(0)2}}{2}. \tag{96}$$

Now, differentiating (96) with respect to x, we obtain

$$P_{xx}^{(0)} + 6\frac{h_x}{\ell^{(0)}} P_x^{(0)} = 0,$$

that is the integro-differential equation

$$P_{xx}^{(0)} + \frac{6h_x}{\left[3h + \dfrac{2\int_0^1 P_x^{(0)} h\,dx - \mathsf{Bn}}{\Delta P\,(t)}\right]} P_x^{(0)} = 0. \tag{97}$$

The boundary conditions are $P^{(0)}\big|_{x=0} = \Delta P$, and $P^{(0)}\big|_{x=1} = 0$. The solution $P^{(0)}$ of (97) is then used to evaluate the $v_1^{(0)}$ via (87), $v_2^{(0)}$ via (88) and the yield surface $\sigma^{(0)}$ via (93).

Remark 7 From (92) we observe that $\sigma_x^{(0)} = -2h_x$, meaning that the amplitude of the rigid core becomes larger as the channel narrows, whereas it shrinks as the channel becomes wider. This is in accordance with what found in [21].

5.6 Flow Condition

Let us investigate the conditions on ΔP that prevent the system from coming to a halt. Let $h\,(x) \equiv h_{in}$. From (93) we get:

- $\Delta P > \dfrac{\mathsf{Bn}}{h_{in}}, \Longrightarrow \sigma^{(0)} < h_{in}$ (the fluid is flowing)
- $\Delta P < \dfrac{\mathsf{Bn}}{h_{in}}, \Longrightarrow \sigma^{(0)} > h_{in}$ (no flow)

When $h(x)$ is not uniform we have to ensure that $\sigma^{(0)} < h(x)$, in order to prevent the flow from stopping. Recalling (95) we must impose

$$\ell^{(0)} \geq 3h_{min} - 2h_{in} - \frac{\mathsf{Bn}}{\Delta P} - \frac{2}{\Delta P}\int_0^1 P^{(0)} h_x dx, \tag{98}$$

where $h_{\min} = \min_{x\in[0,1]} h$. To estimate the integral in the r.h.s. we remark that $P^{(0)}$ fulfils Eq. (97), that is an equation of elliptic type. Maximum principle entails $0 \leq P^{(0)} \leq \Delta P$. So, writing

$$\int_0^1 P^{(0)} h_x dx = \underbrace{\int_{\{h_x\leq 0\}} P^{(0)} h_x dx}_{\leq 0} + \underbrace{\int_{\{h_x\geq 0\}} P^{(0)} h_x dx}_{\geq 0},$$

we have

$$\Delta P \min\left\{\underline{h}_x; 0\right\} \leq \Delta P \max\left\{\overline{h}_x; 0\right\},$$

where

$$\underline{h}_x = \min_{x\in[0,1]} h_x(x), \quad \text{and} \quad \overline{h}_x = \min_{x\in[0,1]} h_x(x).$$

In conclusion

$$2\min\left\{\underline{h}_x; 0\right\} \leq \frac{2}{\Delta P}\int_0^1 P^{(0)} h_x dx \leq 2\max\left\{\overline{h}_x; 0\right\}. \tag{99}$$

Therefore, recalling (98), we have

$$\begin{aligned}\ell^{(0)} &\geq 3h_{\min} - 2h_{in} - \frac{\mathsf{Bn}}{\Delta P} - \frac{2}{\Delta P}\int_0^1 P^{(0)} h_x dx \\ &\geq 3h_{\min} - 2\max\left\{\overline{h}_x; 0\right\} - 2h_{in} - \frac{\mathsf{Bn}}{\Delta P},\end{aligned} \tag{100}$$

If we assume

$$\left(3h_{\min} - 2\max\left\{\overline{h}_x; 0\right\} - 2h_{in}\right) > 0$$

and require that

$$3h_{\min} - 2\max\left\{\overline{h}_x; 0\right\} - 2h_{in} - \frac{\mathsf{Bi}}{\Delta P} > 0,$$

which implies

$$\Delta P > \frac{\mathsf{Bn}}{3h_{\min} - 2\max\left\{\overline{h}_x; 0\right\} - 2h_{in}}, \tag{101}$$

we are sure that the flow never comes to a stop.

Example 2 If we consider a linear wall profile

$$h = h_{in} + \underbrace{(h_{out} - h_{in})}_{\Delta h} x,$$

where $h_{out} > 0$, there are two possibilities:

- $\Delta h > 0, \Rightarrow h_{\min} = h_{in}$, and $\max\left\{\overline{h}_x; 0\right\} = \Delta h$. Condition (101) yields

$$\frac{\mathsf{Bn}}{\Delta P} < \underbrace{h_{in} - 2\Delta h}_{2h_{out} - 3h_{in}}, \quad \Leftrightarrow \quad \Delta P > \frac{\mathsf{Bn}}{2h_{out} - 3h_{in}},$$

  where, of course, we assume $2h_{out} - 3h_{in} > 0$
- $\Delta h < 0, \Rightarrow h_{\min} = h_{out}$, and $\max\left\{\overline{h}_x; 0\right\} = 0$. Inequality (101) entails

$$\frac{\mathsf{Bn}}{\Delta P} < \underbrace{2\Delta h + h_{out}}_{3h_{out} - 2h_{in}}, \quad \Leftrightarrow \quad \Delta P > \frac{\mathsf{Bn}}{3h_{out} - 2h_{in}},$$

  where now we require $3h_{out} - 2h_{in} > 0$.

5.7 Inner Core Appearance or Disappearance

A non uniform channel profile may cause the appearance/disappearance of the rigid plug. These phenomena (highlighted also in [6] and [21]) are not possible when the channel profile is uniform, namely when $h(x) \equiv h_{in}$. Recalling (93), we set

$$\sigma^{(0)} = \max\left\{0;\ 2(h_{in} - h) + \frac{\mathsf{Bn}}{\Delta P} + \frac{2}{\Delta P}\int_0^1 P^{(0)} h_x dx\right\},$$

in order to avoid physical inconsistencies. Hence, $\sigma^{(0)}$ vanishes when

$$h \geq h_{in} + \frac{\mathsf{Bn}}{2\Delta P} + \frac{1}{\Delta P}\int_0^1 P^{(0)} h_x dx. \tag{102}$$

The r.h.s. of (102) is a critical value, that we denote as h_{crt}, such that, whenever $h \geq h_{crt}$ the core disappears.

Example 3 Let us consider the channel profile

$$h(x) = \frac{\arctan\left[5\left(\frac{1}{2} - x\right)\right]}{4\arctan\left(\frac{5}{2}\right)} + \frac{3}{4}. \tag{103}$$

depicted with the dashed line in Fig. 20. We now estimate h_{crt} exploiting (102), when $\Delta P = 10$, and $\mathsf{Bi} = 5$,

$$\begin{aligned} h(x) &\geq 1 + \frac{\mathsf{Bn}}{2\Delta P} - \frac{1}{\Delta P}\int_0^1 P^{(0)}\,|h_x|\,dx \\ &\geq 1 + \frac{\mathsf{Bn}}{2\Delta P} - \|h_x\|_{L^2} \geq 1 + \frac{\mathsf{Bn}}{2\Delta P} - 0.58 \approx 0.67. \end{aligned}$$

The core-free region is thus obtained solving $h \geq h_{crt}$, which we approximate with $h \geq 0.67$, whose solution is the interval $1 \leq x \leq 0.58$. Looking at Fig. 20 the actual core-free region is $1 \leq x \leq 0.55$, which substantially agrees with the above estimate.

5.8 Solution for an Almost Flat Channel

When $h(x) \equiv h_{in}$ (i.e. uniform channel) equation (93) gives

$$\sigma^{(0)} = \frac{\mathsf{Bn}}{\Delta P}. \tag{104}$$

Equation (97) yields

$$P^{(0)} = (1 - x)\,\Delta P.$$

The velocity field becomes[7]

$$\begin{cases} v_1^{(0)} = -\Delta P\left[\dfrac{(y - \sigma^{(0)})^2}{2} - \dfrac{(1 - \sigma^{(0)})^2}{2}\right], \\ v_2^{(0)} = 0, \end{cases} \tag{105}$$

[7] We set, for the sake of simplicity, $h_{in} = 1$.

and we also find

$$k_1^{(0)} = \frac{\Delta P}{2}(1-\sigma^{(0)})^2.$$

Let us now consider a non-uniform channel profile $h(x)$, assuming that amplitude width variation is small. We thus set

$$h(x) = \langle h \rangle + \phi(x), \tag{106}$$

where $\langle h \rangle$ denotes the spatial average along the channel, i.e.

$$\langle h \rangle = \int_0^1 h(x)\, dx$$

and assume that $\max|\phi(x)|$ is small, that is we consider an almost flat channel. We look for $P^{(0)}$ in the form

$$P^{(0)} = (1-x)\,\Delta P + \Pi, \tag{107}$$

where $\Pi|_{x=0} = \Pi|_{x=1} = 0$, and where we expect that both $\max|\Pi|$, $\max|\Pi_x|$ are small. Inserting (107) into (92) we obtain

$$\sigma^{(0)} = \frac{\mathsf{Bn}}{\Delta P} - 2\phi(x) - \frac{2}{\Delta P}\int_0^1 \Pi_x \phi\, dx \approx \frac{\mathsf{Bn}}{\Delta P} - 2\phi(x). \tag{108}$$

Concerning $\ell^{(0)}$ we have

$$\ell^{(0)}(x,t) \approx \langle h \rangle - \frac{\mathsf{Bn}}{\Delta P(t)} + 3\phi(x). \tag{109}$$

Exploiting then (97) we compute the pressure field solving

$$\Pi_{xx} + \frac{6\phi_x}{\ell^{(0)}}(-\Delta P + \Pi_x) = 0.$$

Neglecting $\phi_x \Pi_x$ we end up with the following problem

$$\begin{cases} \Pi_{xx} - 2\Delta P\left[\dfrac{\phi_x}{\phi + \mathscr{A}}\right] = 0, \quad \text{where} \quad \mathscr{A} = \dfrac{< h >}{3} - \dfrac{\mathsf{Bn}}{3\Delta P}, \\ \\ \Pi|_{x=0} = \Pi|_{x=1} = 0, \end{cases}$$

so that

$$\Pi_x = (const) + 2\Delta P \ln\left[1 + \frac{\phi\,(x)}{\mathscr{A}}\right] \approx (const) + 2\Delta P \frac{\phi\,(x)}{\mathscr{A}}.$$

In conclusion

$$\Pi = \frac{2\Delta P\,(t)}{\mathscr{A}} \int_0^x \phi\,(x^{'})dx^{'},$$

which yields

$$P^{(0)} = \Delta P\,(1-x) + \frac{6\Delta P^2}{\langle h\rangle\,\Delta P - \mathsf{Bn}} \int_0^x \phi\left(x'\right) dx'. \tag{110}$$

Example 4 Let us consider $h\,(x) = 1 + mx$, with m small. We write

$$h\,(x) = \underbrace{1 + \frac{m}{2}}_{\langle h\rangle} + \underbrace{m\left(x - \frac{1}{2}\right)}_{\phi(x)}.$$

In this case

$$\sigma^{(0)} = \frac{\mathsf{Bn}}{\Delta P} - 2m\left(x - \frac{1}{2}\right),$$

and

$$P^{(0)} = \Delta P\,(1-x) + \frac{3m\Delta P^2}{\langle h\rangle\,\Delta P - \mathsf{Bn}} x\,(x-1)\,.$$

We see that $\sigma_x^{(0)} = -2m$, i.e. the core amplitude widens for $m < 0$ and shrinks for $m > 0$.

Example 5 Let us consider a wavy channel

$$h(x) = 1 - \theta\cos\left[2\pi\delta\left(x - \frac{1}{2}\right)\right], \tag{111}$$

where $\delta > 0$, and $\theta \ll 1$. We write

$$h\,(x) = \underbrace{\left[1 - \frac{\theta}{\pi\,\delta}\sin\left(\pi\,\delta\right)\right]}_{\langle h\rangle} + \underbrace{\theta\left[\frac{\sin\left(\pi\,\delta\right)}{\pi\,\delta} - \cos\left(2\pi\,\delta\left(x - \frac{1}{2}\right)\right)\right]}_{\phi(x)},$$

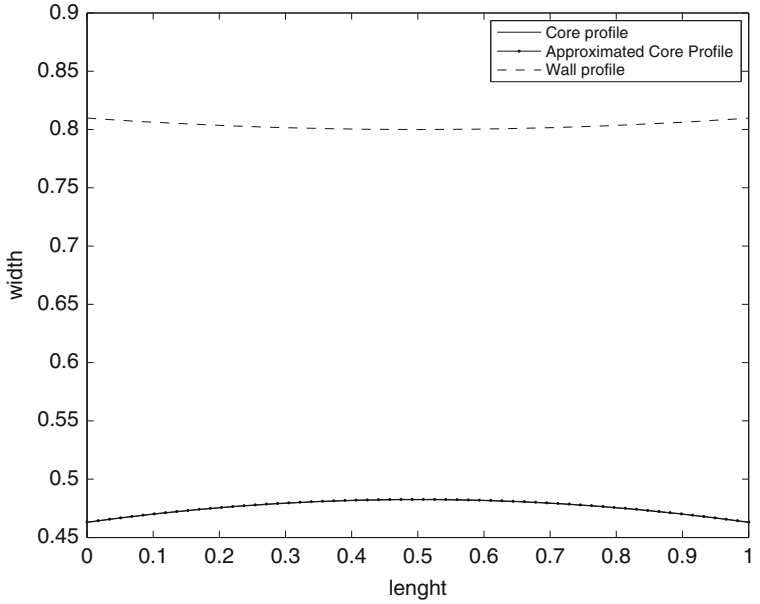

Fig. 16 The channel profile $h(x)$ is (111) and of $\sigma^{(0)}$ given by (92), (112), with $\mathsf{Bn} = 5$, $\Delta P = 10.5$, $\delta = 0.2$, $\theta = 0.1$

with $\max|\phi| = \mathscr{O}(\theta) \ll 1$. Exploiting (108) we obtain

$$\sigma^{(0)} \approx \frac{\mathsf{Bn}}{\Delta P} - 2\theta\left[\frac{\sin(\pi\delta)}{\pi\delta} - \cos\left(2\pi\delta\left(x - \frac{1}{2}\right)\right)\right], \tag{112}$$

The behavior for $\theta = 0.1$, and $\delta = 1/5$ is shown in Figs. 16 and 17. In particular in Fig. 17 a close-up showing the difference between the approximated solution (112) and the computed one (see next section) is displayed.

5.9 Numerical Simulations

Setting $F = P_x^{(0)}$, the elliptic problem (97) can be transformed in the following integral equation

$$F = -\Delta P \frac{\exp\left\{-\int_0^x \frac{6h_{x'}}{\ell_F}dx'\right\}}{\int_0^1 \exp\left\{-\int_0^x \frac{6h_{x'}}{\ell_F}dx'\right\}dx}, \tag{113}$$

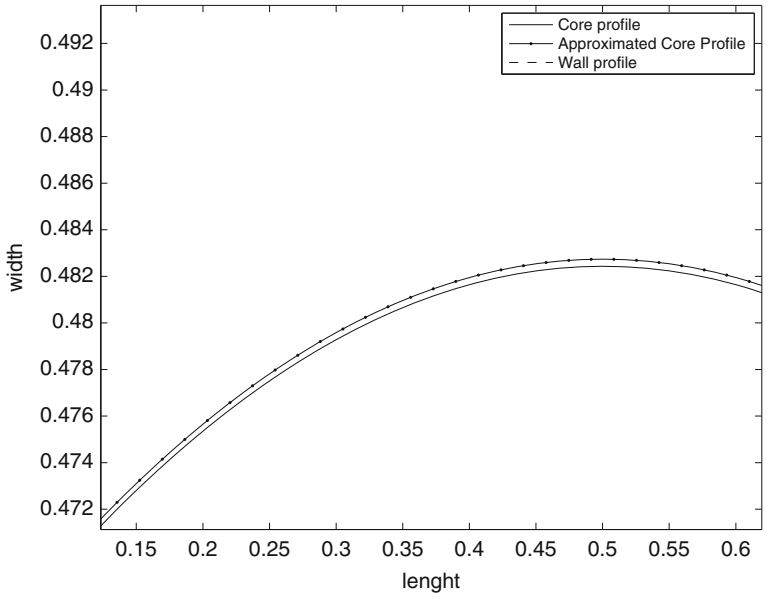

Fig. 17 Close up for the difference between $\sigma^{(0)}$ given by (112) and $\sigma^{(0)}$ given by (92)

where, recalling (95),

$$\ell_F = \min\left\{ h(x)\,,\ 3h(x) + \frac{2\displaystyle\int_0^1 Fh\,dx - \mathsf{Bn}}{\Delta P} \right\}.$$

Now, if the conditions ensuring that $\ell^{(0)}$ is strictly positive (Sect. 5.6) are fulfilled, we can solve (113) through the following iterative procedure:

Step $j = 0$. Set $F_0 = -\Delta P$, and $\ell_{F,\,0} = \min\left\{ h(x)\,,\ 3h(x) - \dfrac{\mathsf{Bn}}{\Delta P} - 2\displaystyle\int_0^1 h\,dx \right\}$.

Step $j = 1$. $F_1 = -\Delta P \dfrac{\exp\left\{ -\displaystyle\int_0^x \frac{6h_{x'}}{\ell_{F,\,0}} dx' \right\}}{\displaystyle\int_0^1 \exp\left\{ -\int_0^x \frac{6h_{x'}}{\ell_{F,\,0}} dx' \right\} dx}$.

.....

Step $j > 1$. $F_j = -\Delta P \dfrac{\exp\left\{ -\displaystyle\int_0^x \frac{6h_{x'}}{\ell_{F,\,j-1}} dx' \right\}}{\displaystyle\int_0^1 \exp\left\{ -\int_0^x \frac{6h_{x'}}{\ell_{F,\,j-1}} dx' \right\} dx}$, with

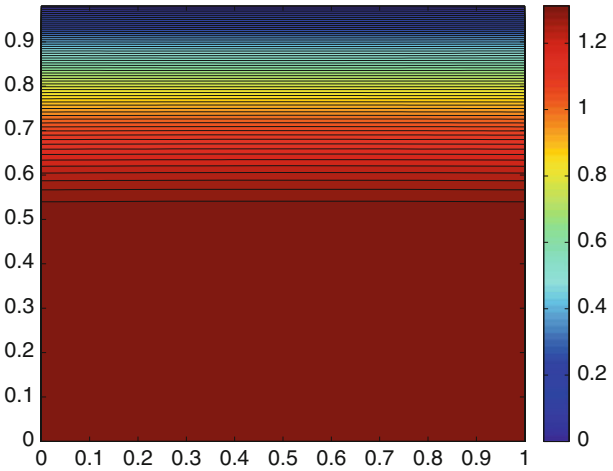

Fig. 18 Plot of x-component of the velocity, h given by (111), $\delta = 0.1$, $\theta = 0.02$, and $\mathsf{Bn} = 5$, $\Delta P = 10.5$

$$\ell_{F,\,j-1} = \min \left\{ h\,(x)\,,\ 3h\,(x) + \frac{2\displaystyle\int_0^1 F_{j-1}\,h\,dx - \mathsf{Bi}}{\Delta P} \right\}.$$

Iterating the procedure until the desired tolerance is reached, we determine the solution $F = P_x^{(0)}$. Integration then provides the pressure field $P^{(0)}$. We can show that, under suitable hypotheses, the solution of (113) exists and is unique.

In Figs. 16, 17 we have plotted $h(x)$ and $\sigma^{(0)}(x)$ for the wavy channel profile given by (111). In Figs. 18, 19 we have reported the contour plots of $v_1^{(0)}$, and $v_2^{(0)}$, when $h(x)$ is given by (111), with $\delta = 0.1$, $\theta = 0.02$, and $\mathsf{Bn} = 5$.
The solid colored regions of Figs. 18 and 19 denote the core, with vanishing transversal velocity and uniform longitudinal velocity. Notice also the symmetry of the transversal velocity shown in Fig. 19. In Figs. 20, 21, 22 we have considered the profile (103). The yield surface $\sigma^{(0)}$ and the velocities $v_1^{(0)}$, $v_2^{(0)}$ are reported respectively.

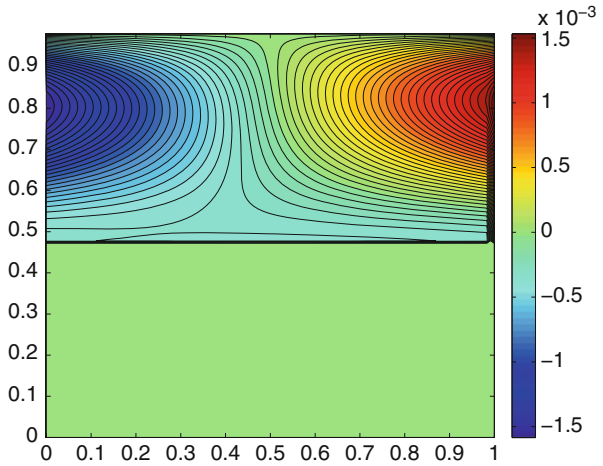

Fig. 19 Plot of y-component of the velocity, h given by (111), $\delta = 0.1$, $\theta = 0.02$, and $\mathsf{Bn} = 5$, $\Delta P = 10.5$

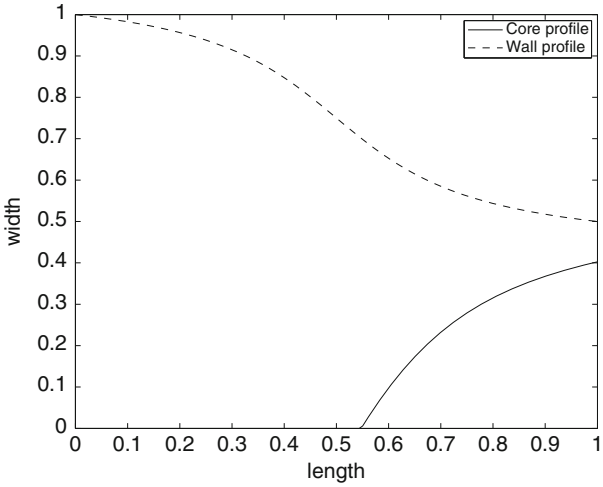

Fig. 20 Plot of $\sigma^{(0)}$ and h, when h is given by (103). $\mathsf{Bn} = 5$, $\Delta P = 10.5$

5.10 Model with Pressure Dependent Viscosity

In this section we extend our model to the case of a pressure-dependent viscosity. Going back to dimensional variables equation (65) rewrites in this way

$$\mathbf{D} = \frac{II_{\mathbf{D}}}{2\mu\,(P)\,II_{\mathbf{D}} + \tau_o}\mathbf{S}.$$

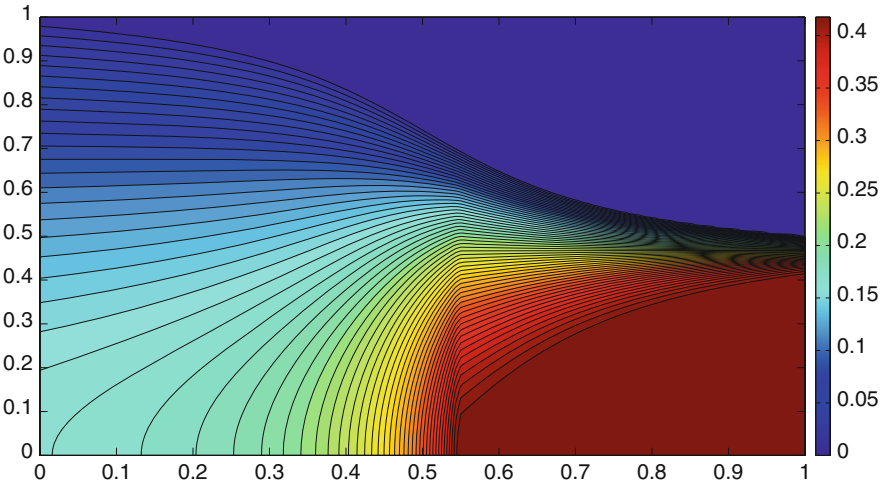

Fig. 21 Plot of x-component of the velocity, h given by (103). $\mathsf{Bn} = 5$, $\Delta P = 10.5$

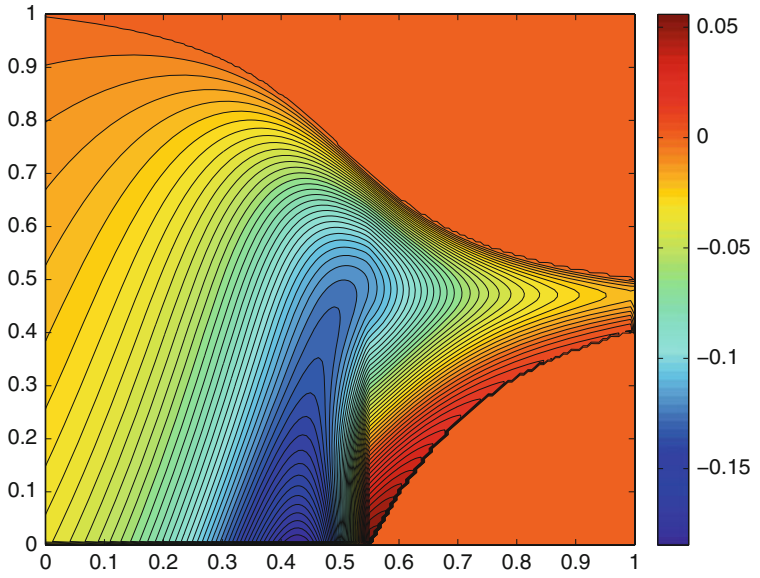

Fig. 22 Plot of y-component of the velocity, h given by (103). $\mathsf{Bn} = 5$, $\Delta P = 10.5$

The viscosity is expanded considering

$$\mu(P) = \mu\Big(P^{(0)} + \varepsilon P^{(1)} + \varepsilon^2 P^{(2)} + \ldots\ldots\Big),$$

so that, around $\varepsilon = 0$, we get $\mu = \mu^{(0)} + \varepsilon\mu^{(1)} + \varepsilon^2\mu^{(2)} + \ldots$, where

$$\mu^{(0)} = \mu(P^{(0)}), \qquad \mu^{(1)} = \frac{d\mu}{dP}(P^{(0)})\, P^{(1)}. \tag{114}$$

Following the same procedure described in Sect. 5.5, the non-dimensional leading order problem becomes

$$\begin{cases} \dfrac{\partial v_1^{(0)}}{\partial x} + \dfrac{\partial v_2^{(0)}}{\partial y} = 0, \\ -\dfrac{\partial P^{(0)}}{\partial x} + \dfrac{\partial}{\partial y}\left(\mu^{(0)}\left(P^{(0)}\right)\dfrac{\partial v_1^{(0)}}{\partial y}\right) = 0, \\ -\dfrac{\partial P^{(0)}}{\partial y} = 0, \end{cases}$$

whose boundary conditions are still given by (86). We get

$$\begin{cases} v_1^{(0)} = \dfrac{P_x^{(0)}}{\mu^{(0)}\left(P^{(0)}\right)} \dfrac{(y - h^{(0)})(y - 2\sigma^{(0)} + h^{(0)})}{6}, \\ v_2^{(0)} = \dfrac{\partial}{\partial x}\left[\dfrac{P_x^{(0)}}{\mu^{(0)}\left(P^{(0)}\right)} \dfrac{(y - h^{(0)})^2(y - 3\sigma^{(0)} + 2h^{(0)})}{6}\right], \end{cases}$$

and

$$k_1^{(0)} = -\frac{P_x^{(0)}}{\mu(P^{(0)})} \frac{(h^{(0)} - \sigma^{(0)})^2}{2}.$$

The interface $\sigma^{(0)}$ is still given by (92), while Eq. (97) modifies in this way

$$\left(\frac{P_x^{(0)}}{\mu(P^{(0)})}\right)_x + 6\frac{h_x}{\ell^{(0)}} \frac{P_x^{(0)}}{\mu(P^{(0)})} = 0, \tag{115}$$

where $\ell^{(0)}$ is given by (95).

Example 6 In case $\mu(P) = e^{\gamma P}$, and $h \equiv 1$, we get

$$\begin{cases} v_1^{(0)} = \dfrac{[e^{-\gamma P_{in}} - e^{-\gamma P_{out}}]}{\gamma} \left[\dfrac{(y - \sigma^{(0)})^2}{2} - \dfrac{(1 - \sigma^{(0)})^2}{2} \right], \\ v_2^{(0)} = 0, \\ \sigma^{(0)} = \dfrac{\mathsf{Bn}}{\Delta P}, \\ P = P_{in} - \dfrac{1}{\gamma} \ln \left[1 + \left(e^{\gamma \Delta P} - 1 \right) x \right]. \end{cases} \tag{116}$$

We now consider $h^{(0)} = 1 + mf(x)$, with m small perturbation. We look for a solution of (115) of the form

$$P^{(0)} = P_{in} - \frac{1}{\gamma} \ln \left[1 + \left(e^{\gamma \Delta P} - 1 \right) x \right] + m\Pi, \tag{117}$$

with $\Pi = 0$ on $x = 0, 1$. After inserting (117) into (115) and neglecting the m^2, we find

$$\Pi = -\frac{6}{\gamma} \frac{\left(e^{\gamma \Delta P} - 1 \right)}{1 + \left(e^{\gamma \Delta P} - 1 \right) x} \left[x \int_0^1 f(\xi) d\xi - \int_0^x f(\xi) d\xi \right],$$

and

$$\sigma^{(0)} = \frac{\mathsf{Bn}}{\Delta P} - m \left[2f(x) - \frac{2}{\gamma \Delta P} \int_0^1 \frac{f(\xi) \left(e^{\gamma \Delta P} - 1 \right)}{1 + \left(e^{\gamma \Delta P} - 1 \right) \xi} d\xi \right].$$

6 Planar Squeeze

We consider the flow of an incompressible Bingham fluid placed between parallel plates of length in a channel of length L. The gap between the plates occupied by the fluid has amplitude $2h(t)$, as depicted in Fig. 23 (see also [19]). Because of symmetry, we confine our analysis to the upper part of the layer, namely $[0, h(t)]$. The velocity field is $\mathbf{v} = u(x, y, t)\mathbf{i} + v(x, y, t)\mathbf{j}$, where x, y are the longitudinal and transversal coordinate respectively.

We assume that the region where $II_{\mathbf{S}} \geq \tau_o$ (yielded) and the region where $II_{\mathbf{S}} \leq \tau_o$ (unyielded) are separated by a sharp interface $y = \pm Y(x, t)$ representing the yield surface. We also define the inner plug

$$\Omega_p = \{(x, y) : \quad x \in [0, L], \quad y \in [-Y, Y]\}.$$

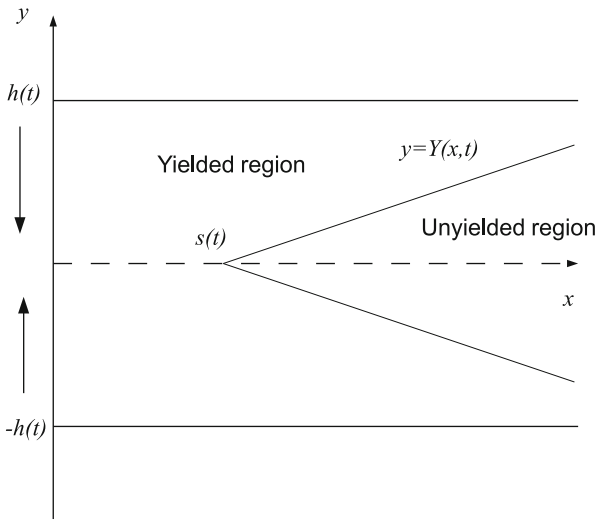

Fig. 23 A schematic representation of the squeezing channel

We may have $Y(x, t) = 0$ for some $x \in (0, L)$ and for some t, so that Ω_p becomes a segment of zero measure. The rigid plug Ω_p moves uniformly with velocity

$$\begin{cases} u = u_p(t), \\ \\ v = 0, \quad \text{(by symmetry)}. \end{cases} \tag{118}$$

Neglecting inertia and body forces, the governing equations in the viscous phase are

$$\text{tr}\mathbf{D} = 0,$$

and

$$-\frac{\partial P}{\partial x} + \frac{\partial S_{11}}{\partial x} + \frac{\partial S_{12}}{\partial y} = 0, \tag{119}$$

$$-\frac{\partial P}{\partial y} + \frac{\partial S_{12}}{\partial x} + \frac{\partial S_{22}}{\partial y} = 0, \tag{120}$$

The integral momentum balance for the domain Ω_p is given by

$$\int_{\Omega_p} \frac{\partial}{\partial t} (\rho \mathbf{v})\, dV + \int_{\partial\Omega_p} \rho \mathbf{v}\, (\mathbf{v} \cdot \mathbf{n})\, dS = \int_{\partial\Omega_p} (\mathbf{Tn}) dS, \tag{121}$$

where ρ is the material density. Neglecting the inertial terms, we get following equation[8]

$$\int_0^L [-Y_x T_{11} + T_{12}]_{Y^+} \, dx + P_{Y_0} Y_0 - P_{Y_1} Y_1 = 0. \tag{122}$$

where P_{Y_o}, P_{Y_1} represent the normal stresses on $x = 0$ and $x = L$. As usual we impose

$$\boldsymbol{v}|_{y=h} \cdot \mathbf{t} = 0, \qquad \left(\mathbf{v}|_{y=h} - \mathbf{w}\right) \cdot \mathbf{n} = 0, \tag{123}$$

where $\mathbf{w} \cdot \mathbf{n}$ is the wall normal velocity and $\mathbf{t}$ is the wall tangent vector. On Y we write

$$[\![\mathbf{v}]\!]_{y=Y} = 0, \tag{124}$$

$$[\![\mathbf{Tn} \cdot \mathbf{t}]\!]_{y=Y} = 0, \qquad [\![\mathbf{Tn} \cdot \mathbf{n}]\!]_{y=Y} = 0, \tag{125}$$

while at $x = 0$

$$\begin{cases} u = 0, \\ \\ S_{12} = 0, \end{cases} \tag{126}$$

6.1 Squeezing Between Parallel Plates

We assume $h = h\,(t)$ and we set

$$H = \max_{t \geq 0} h(t).$$

We define the aspect ratio $\varepsilon = H/L$, assuming $\varepsilon \ll 1$. Then we rescale the problem using the following non dimensional variables

$$\tilde{x} = \frac{x}{L}, \qquad \tilde{y} = \frac{y}{\varepsilon L}, \qquad \tilde{Y} = \frac{Y}{\varepsilon L}, \qquad \tilde{h} = \frac{h}{H}, \qquad \tilde{t} = \frac{t}{T},$$

where T is the characteristic time scale, i.e. the "squeezing time". We define the characteristic transversal velocity as $V = H/T$, and the longitudinal velocity as $U = V/\varepsilon$, so that $u = u/U$, $v = v/V = v^*/(\varepsilon U)$. Pressure is again rescaled

[8]The expression $[-Y_x T_{11} + T_{12}]_{Y^+}$ represents the force exerted by the viscous region on the lateral side of the inner rigid core.

exploiting the Poiseuille formula $P_c = (\mu LU)/H^2$ and we set $P = P/P_c$, $P_{out} = P_{out}/P_c$, where P_{out} is the (given) pressure field applied at the channel outlet. We suppose that P_{out} is constant in time and space. Next we introduce

$$\mathbf{S} = \frac{\mathbf{S}}{(\mu U/H)}, \qquad \mathbf{D} = \frac{\mathbf{D}}{(U/H)}, \qquad \mathit{II}_{\mathbf{D}} = \frac{\mathit{II}_{\mathbf{D}}}{(U/H)}, \qquad \mathit{II}_{\mathbf{S}} = \frac{\mathit{II}_{\mathbf{S}}}{(\mu U/H)},$$

so that

$$\mathbf{S} = \left(2 + \frac{\mathsf{Bn}}{\mathit{II}_D}\right)\mathbf{D},$$

where

$$\mathsf{Bn} = \frac{\tau_o H}{\mu U}$$

is again the Bingham number. The mechanical incompressibility constraint and momentum balance become (neglect the tildas)

$$\frac{\partial u}{\partial x} + \frac{\partial v}{\partial y} = 0, \tag{127}$$

$$-\frac{\partial P}{\partial x} + \varepsilon \frac{\partial S_{11}}{\partial x} + \frac{\partial S_{12}}{\partial y} = 0, \tag{128}$$

$$-\frac{\partial P}{\partial y} + \varepsilon^2 \frac{\partial S_{12}}{\partial x} + \varepsilon \frac{\partial S_{22}}{\partial y} = 0. \tag{129}$$

Equation (122) can be rewritten as

$$\int_0^1 [PY_x - \varepsilon Y_x S_{11} + S_{12}]_{Y^+}\, dx + P_{Y_0} Y_0 - P_{out} Y_1 = 0, \tag{130}$$

where $P_{out} = P_{Y_1}$. Boundary conditions (123) become

$$u|_h = 0, \qquad v|_h = \dot{h}, \tag{131}$$

since the squeezing velocity is

$$\dot{h} = \frac{\partial h}{\partial t} < 0$$

Jump conditions on Y become

$$[\![u]\!]_{y=Y} = [\![v]\!]_{y=Y} = 0, \tag{132}$$

$$\begin{cases} [\![P]\!]\left[1+\varepsilon^2\left(\dfrac{\partial Y}{\partial x}\right)^2\right]_{y=Y} + \left[\varepsilon^3 S_{11}\left(\dfrac{\partial Y}{\partial x}\right)^2 - 2\varepsilon^2 S_{12}\left(\dfrac{\partial Y}{\partial x}\right) + \varepsilon S_{22}\right]_{y=Y} = 0, \\ [\![S_{12}]\!]_{y=Y} + \varepsilon\left(\dfrac{\partial Y}{\partial x}\right)\left[S_{22} - S_{11} - \varepsilon S_{12}\dfrac{\partial Y}{\partial x}\right]_{y=Y} = 0, \end{cases} \tag{133}$$

while conditions (126) become

$$\begin{cases} u = 0, \\ S_{12} = 0. \end{cases} \tag{134}$$

6.2 Problem at the Leading Order

As for the channel, we look for a solution expressed as power series of ε, assuming $\mathsf{Bi} = \mathscr{O}(1)$. We get

$$S_{12}^{(0)} = u_y^{(0)} - \mathsf{Bn}$$

since we are looking for a solution with $u_y^{(0)} < 0$ in the upper part of the channel. Equations (127)–(129) reduces to

$$\begin{cases} \dfrac{\partial u^{(0)}}{\partial x} + \dfrac{\partial v^{(0)}}{\partial y} = 0, \\ -\dfrac{\partial P^{(0)}}{\partial x} + \dfrac{\partial}{\partial y}\left(\dfrac{\partial u^{(0)}}{\partial y}\right) = 0, \\ -\dfrac{\partial P^{(0)}}{\partial y} = 0, \end{cases} \tag{135}$$

with boundary conditions

$$\begin{cases} \left.\dfrac{\partial u^{(0)}}{\partial y}\right|_{y=Y} = 0 \\ u^{(0)}(x, h, t) = 0 \end{cases} \tag{136}$$

For the sake of simplicity we suppress the superscript (0). Since $P = P(x, t)$ we get

$$u = -P_x \frac{(h-y)(y-2Y+h)}{2}. \tag{137}$$

Moreover exploiting mass conservation

$$\dot{h} - v(y,t) = \int_y^h \frac{\partial}{\partial x}\left[P_x \frac{(h-y')(y'-2Y+h)}{2}\right] dy'.$$

Evaluating u, v on Y and recalling conditions (132), we obtain

$$u_p(t) = -P_x \frac{(Y-h)^2}{2}, \tag{138}$$

$$v|_{y=Y} = \dot{h} + \frac{\partial}{\partial x}\left[P_x \frac{(Y-h)^3}{3}\right] - \frac{Y_x}{2} P_x (Y-h)^2 = 0. \tag{139}$$

The plug equation (130) becomes

$$-\int_0^1 P_x Y dx = \mathsf{Bn}. \tag{140}$$

Recalling (134) we have $u_y = 0$ in $x = 0$ implying $P_x|_{x=0} = 0$. The solid region must be detached from $x = 0$, since otherwise $u_p \equiv 0$, i.e. no rigid domain motion. Accordingly there must be some $s(t) \in [0, 1]$, not a priori known, such that $Y(x, t) \equiv 0$, for $0 \le x \le s(t)$. Hence the spatial domain $[0, 1]$ can be split in two sub-domains (see Fig. 23):

- $0 \le x \le s(t)$, where $Y \equiv 0$;
- $s(t) < x \le 1$, where Y does not vanish.

Assuming that the longitudinal velocity is continuous across $s(t)$, we have

$$u_p(t) = -\frac{P_x(s,t)}{2}(\underbrace{Y(s,t)}_{0} - h)^2 = -\frac{P_x(s,t)}{2} h^2, \tag{141}$$

where $P_x(s, t)$ is unknown at this stage. From (139) we get

$$-\dot{h} + \frac{2}{3}\frac{\partial}{\partial x}\Big[\underbrace{-\frac{P_x}{2}(Y-h)^2}_{u_p(t)}(Y-h)\Big] - Y_x \underbrace{\Big[-\frac{P_x}{2}(Y-h)^2\Big]}_{u_p(t)} = 0,$$

that is

$$\dot{h} + \frac{1}{3} u_p(t) Y_x = 0, \tag{142}$$

In order to avoid physical inconsistencies, we set

$$Y(x,t) = \max\left\{0, -\frac{3\dot{h}s(t)}{u_p(t)}\left(\frac{x}{s(t)} - 1\right)\right\}. \tag{143}$$

The local instantaneous discharge is given by

$$Q(x,t) = \int_0^Y u_p dy + \int_Y^h u dy = u_p Y - \frac{P_x(x,t)}{3}(h-Y)^3. \tag{144}$$

Mass conservation then requires $Q(x,t) = -\dot{h}x$, so that $Q(s,t) = -\dot{h}s$ so that

$$u_p(t) = -\frac{3}{2}\frac{\dot{h}}{h}s, \tag{145}$$

which is positive since $\dot{h} < 0$. As a consequence

$$Y(x,t) = \max\left\{0,\ 2h(t)\left(\frac{x}{s(t)} - 1\right)\right\}. \tag{146}$$

Therefore the fluid squeezes out of the channel only if $Y(1,t) < h(t)$, namely when $s(t) > 2/3$. In $x \in [0,s]$ we have $Y = 0$ and the pressure fulfills Eq. (139) with the boundary condition $P_x(0,t) = 0$

$$\begin{cases} P_{xx} = \dfrac{3}{h^3}\dot{h}, \quad 0 < x < s, \quad t \geq 0 \\ \\ P_x(0,t) = 0 \ t \geq 0. \end{cases}$$

Therefore

$$P(x,t) = \frac{3\dot{h}}{2h^3}x^2 + A(t),$$

with $A(t)$ still unknown at this stage. Recalling that Y is linear in x we integrate (138) between x and 1 getting

$$P(x,t) = P_{out} + \frac{3}{2}\dot{h}\left(\frac{s}{h}\right)^3\left[\frac{1}{2-3s} - \frac{1}{2x-3s}\right], \qquad s(t) < x \leq 1. \tag{147}$$

Then imposing the continuity of P across $x = s$ we get

$$P(x,t) = \frac{3\dot{h}}{2h^3}\left(x^2 - s^2\right) + P_{out} - 3\dot{h}\frac{s^2}{h^3}\left(\frac{s-1}{2-3s}\right), \qquad 0 \leq x \leq s(t). \tag{148}$$

Finally rewriting (140) as

$$\int_s^1 P_x Y dx = -\mathrm{Bn},$$

we get

$$f(s) = s^2 \left[\frac{2\,(1-s)}{3s-2} + \ln\left(\frac{3s-2}{s}\right)\right] = -\frac{2}{3}\frac{\mathrm{Bn}h^2}{\dot{h}}. \tag{149}$$

Hence, solving (149) we find $s\,(t)$ and we are able to determine the pressure field in the whole channel and the rigid domain as well. We observe that $s(t)$ is not a material point so that, in principle, $s(t)$ can also be still (i.e. $\dot{s}(t) = 0$), while the rigid plug is moving with velocity $u_p(t)$. Figure 24 shows the behavior of the function $f(s)$ in the l.h.s. of (149) with $s \in (2/3, 1)$. We easily realize that $f(s)$ is monotonically decreasing for $2/3 < s \leq 1$ and that its range is $[0, +\infty)$. So, given any $-(2\mathrm{Bn}h^2)/(3\dot{h}) > 0$, there exists one and only one s fulfilling (149). The force acting on the unit surface of upper plate is

$$P\,(t) = \int_0^1 P\,(x,\,t)\,dx = P_{out} + \frac{\dot{h}s^3}{2h^3}\frac{5-3s}{2-3s} - \frac{3\dot{h}s^3}{4h^3}\ln\left(\frac{3s-2}{s}\right).$$

Exploiting (149) we get

$$P\,(t) - P_{out} = \frac{\mathrm{Bn}}{2}\frac{s}{h} - \dot{h}\left(\frac{s}{h}\right)^3 \frac{1}{(3s-2)}. \tag{150}$$

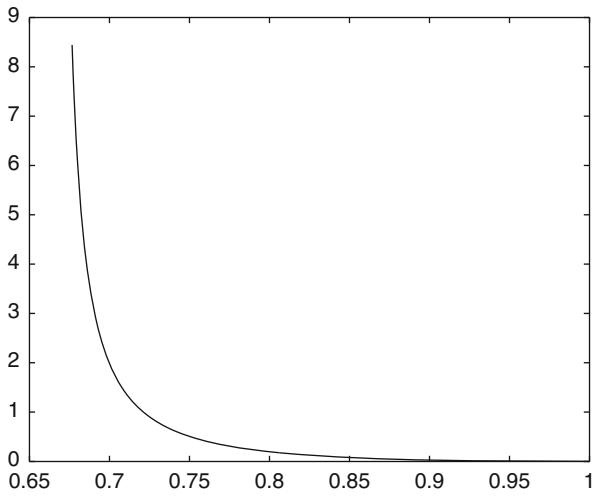

Fig. 24 Behavior of $f\,(s)$ for $2/3 < s \leq 1$

Remark 8 When $\mathsf{Bn} \to 0$, the solution of (149) is simply $s = 1$, i.e. the solid region does not exists at all (as physically expected for a Newtonian fluid). Furthermore formula (150) reduces to

$$P(t) - P_{out} = -\frac{\dot{h}}{h^3},$$

corresponding to the Newtonian fluid planar squeezing, [17]. These results confirms the physical consistency of our model.

6.3 Numerical Simulation

We perform here some numerical simulations to investigate the behavior of our asymptotic solution at the leading order. To illustrate the dependence of the solution on the Bingham number we consider the cases: $\mathsf{Bn} = 1$ and $\mathsf{Bn} = 25$. We plot the yield surface Y, the pressure field P and the axial velocity u, assuming that the plates have constant velocity so that

$$h(t) = 1 - t, \qquad \dot{h}(t) = -1. \tag{151}$$

We consider $t \in [0, 0.6]$, which guarantees that the plates do not come in touch in the select time interval. We set $h_f = h(0.6)$, representing the half gap width at time $t_f = 0.6$ and $s_f = s(0.6)$ representing the onset of the rigid plug at time $t = 0.6$. The yield surface Y and pressure field P are plotted for different times t belonging to the selected time interval and for $x \in [0, 1]$. The axial velocity u is plotted at time $t = 0.6$ (i.e. when $h = h_f$) for a finite number of $x \in [s_f, 1]$ and for y ranging in $[0, h_f]$.

In Figs. 25, 26 we have plotted the yield surface $Y(x, t)$ and the upper plate $y = h(t)$ at different times in the time interval $[0, t_f]$. We have plotted the upper plate only for $x \in [s(t), 1]$ so that the evolution of the onset of the plug $x = s(t)$ is visible. We notice that the slope of the unyielded plug becomes smaller as $s(t)$ increases, as expected. In Figs. 27, 28 we have plotted the pressure field at different times in the time interval $[0, t_f]$ in the whole domain $x \in [0, 1]$. Also for this case the position $x = s(t)$ has been put in evidence. We notice that the pressure within the gap increases as Bn increases.

In Figs. 29, 30 we have plot the axial velocity profile at time $t = 0.6$ for some fixed $x \in [s_f, 1]$. In particular velocity is plotted for $x = 0.69$, $x = 0.73$, $x = 0.77$, $x = 0.81$, $x = 0.85$. As one can easily observe the velocity of the plug is the same for each (x, y) belonging to the plug.

Finally in Figs. 31, 32 we have plotted the squeeze force given in (150) for different values of the Bingham number, Bn. We have plotted (150) for the linear

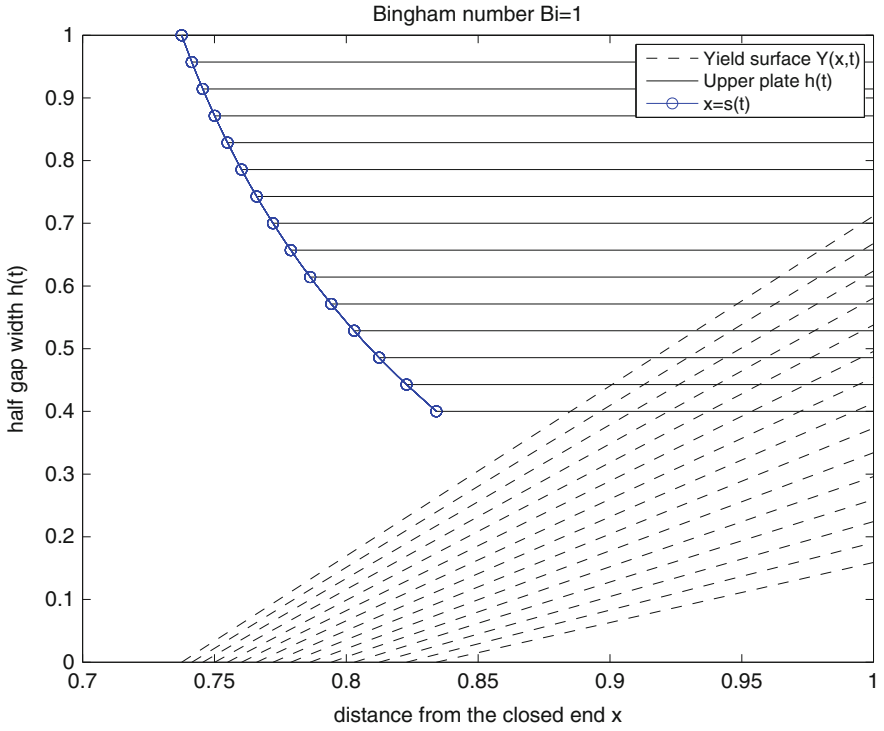

Fig. 25 Y for $\mathsf{Bn} = 1$ and h given by (151)

squeezing (151) and for the exponential squeezing

$$h(t) = \exp(-t), \qquad \dot{h}(t) = -\exp(-t). \tag{152}$$

We observe that the linear squeezing requires a grater squeezing force than the exponential squeezing. This is physically consistent, since in the linear case the plates move faster than in the exponential case.

6.4 Squeezing Between Surfaces

In this section we generalize the problem to the case in which the parallel plates are surfaces $y = \pm h(x, t)$ that are approaching the channel centerline, as shown in Fig. 33. In this case

$$H = \max_{\substack{x\in[0,L]\\ t>0}} h(x, t),$$

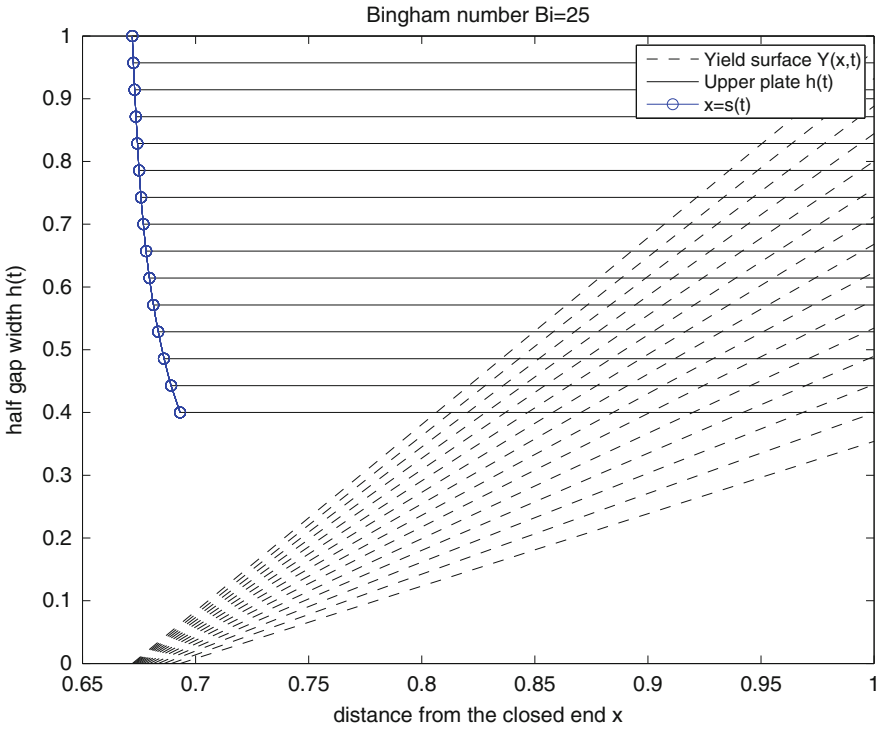

Fig. 26 Y for $\mathsf{Bn} = 25$ and h given by (151)

and we again assume $H/L = \varepsilon \ll 1$. The theory develops exactly as in Sect. 6.1, so that (140) still holds. We split $[0, 1]$ into $[0, s]$ and $[s, 1]$, so that continuity of u across $s\,(t)$ yields

$$u_p(t) = -\frac{P_x\,(s,t)}{2} h(s,t)^2.$$

Recalling (139) we find

$$h_t + \frac{1}{3} u_p(t) Y_x + \frac{2}{3} u_p(t) h_x = 0,$$

which generalizes (142). We thus get the following Cauchy problem

$$\begin{cases} Y_x = \dfrac{3}{u_p}\left[-h_t - \dfrac{2}{3} u_p h_x\right], \\ \\ Y(s,t) = 0, \end{cases}$$

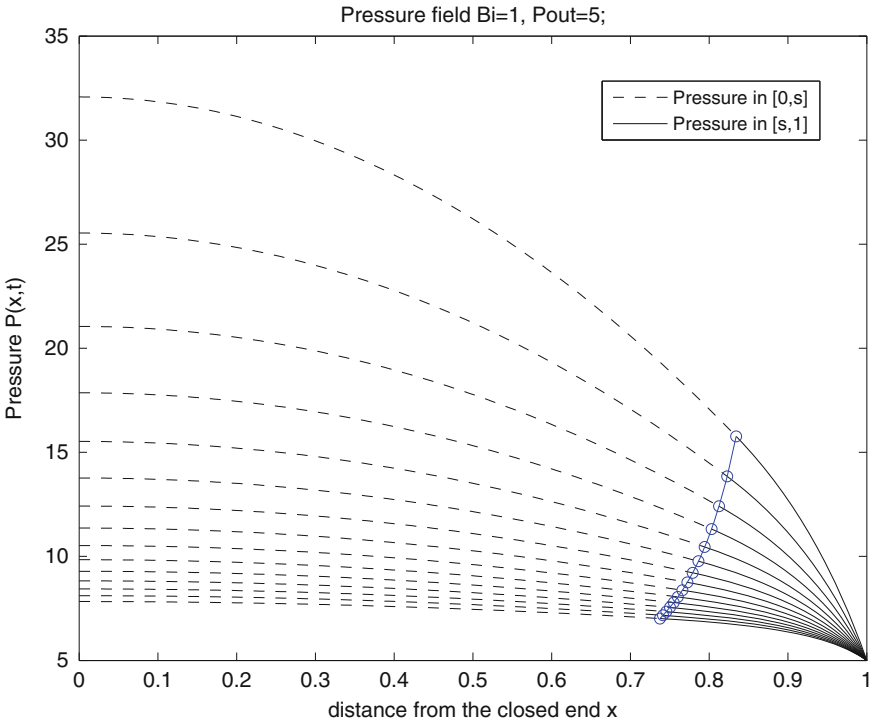

Fig. 27 P for $\mathsf{Bn} = 1$ and h given by (151)

whose solution is

$$Y(x,t) = \frac{3}{u_p}\left[-\int_s^x h_t d\xi - \frac{2}{3}u_p(h(x,t) - h(s,t))\right], \tag{153}$$

where s is still unknown. Following (143) we set

$$Y(x,t) = \max\left\{0,\ -\frac{3}{u_p}\int_s^x h_t d\xi - 2(h(x,t) - h(s,t))\right\}. \tag{154}$$

The local discharge is

$$Q(x,t) = \underbrace{\int_0^Y u_p dy}_{u_p Y} + \underbrace{\int_Y^h \left[-P_x \frac{(h-y)(y-2Y+h)}{2}\right] dy}_{-\frac{P_x(x,t)}{3}(h-Y)^3},$$

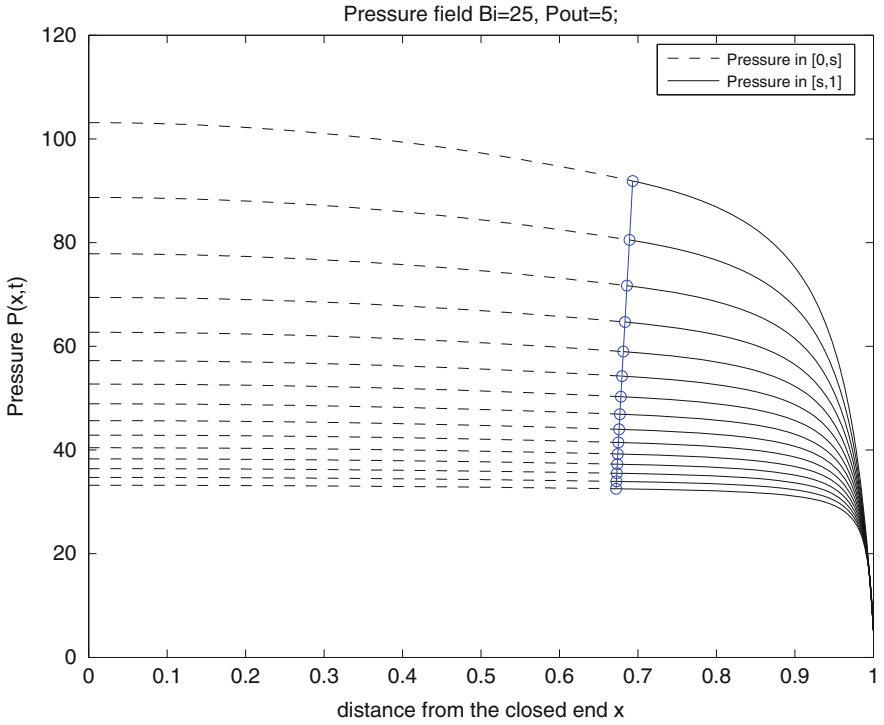

Fig. 28 P for $\mathsf{Bn} = 25$ and h given by (151)

while mass conservation $h_t + Q_x = 0$ implies

$$Q(x,t) = -\int_0^x h_t d\xi,$$

since $Q(0,t) = 0$. We find

$$Q(s,t) = -\int_0^s h_t d\xi = \underbrace{-\frac{P_x(s,t)h^2(s,t)}{2}}_{u_p} \frac{2h(s,t)}{3},$$

implying

$$u_p(t) = -\frac{3}{2}\frac{1}{h(s,t)}\int_0^s h_t d\xi, \tag{155}$$

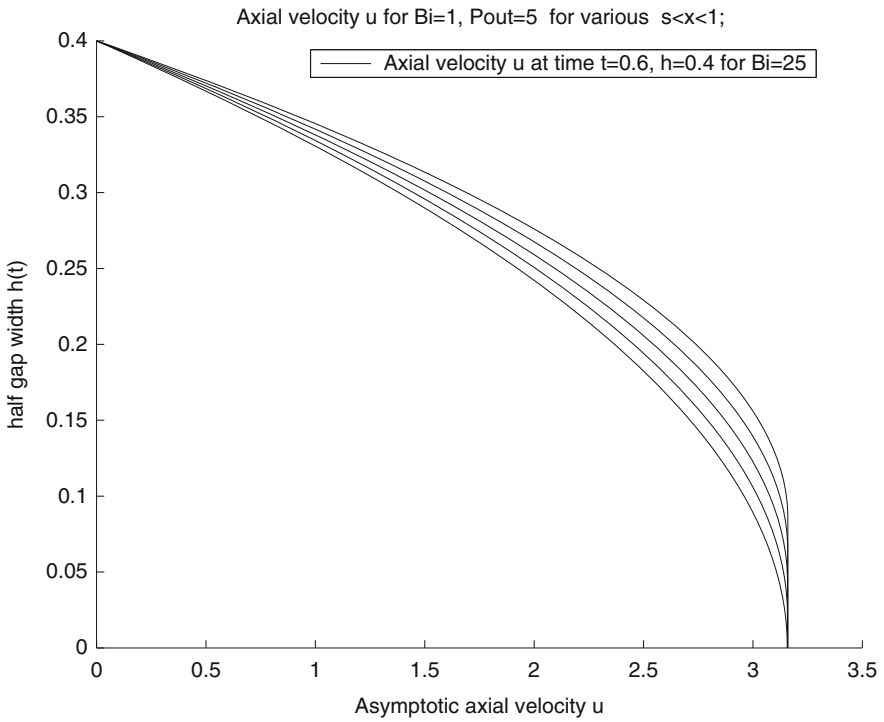

Fig. 29 u for $\mathsf{Bn} = 1$ and h given by (151)

which is the generalization of (145). In conclusion, substituting (155) into (154), we find

$$Y(x,t) = \max\left\{0, \ -2h(x,t) + 2h(s,t)\frac{\int_0^x h_t d\xi}{\int_0^s h_t d\xi}\right\}. \tag{156}$$

In $x \in [0, s]$ the pressure fulfils

$$\begin{cases} -h_t + \dfrac{\partial}{\partial x}\left[P_x \dfrac{h^3}{3}\right] = 0, & 0 < x < s(t), \\ & t \geq 0, \\ P_x(0,t) = 0, & t \geq 0, \end{cases} \tag{157}$$

so that

$$P(x,t) = \int_0^x \left[\frac{3}{h(\tilde{x},t)^3}\int_0^{\tilde{x}} h_t d\xi\right] d\tilde{x} + A(t), \tag{158}$$

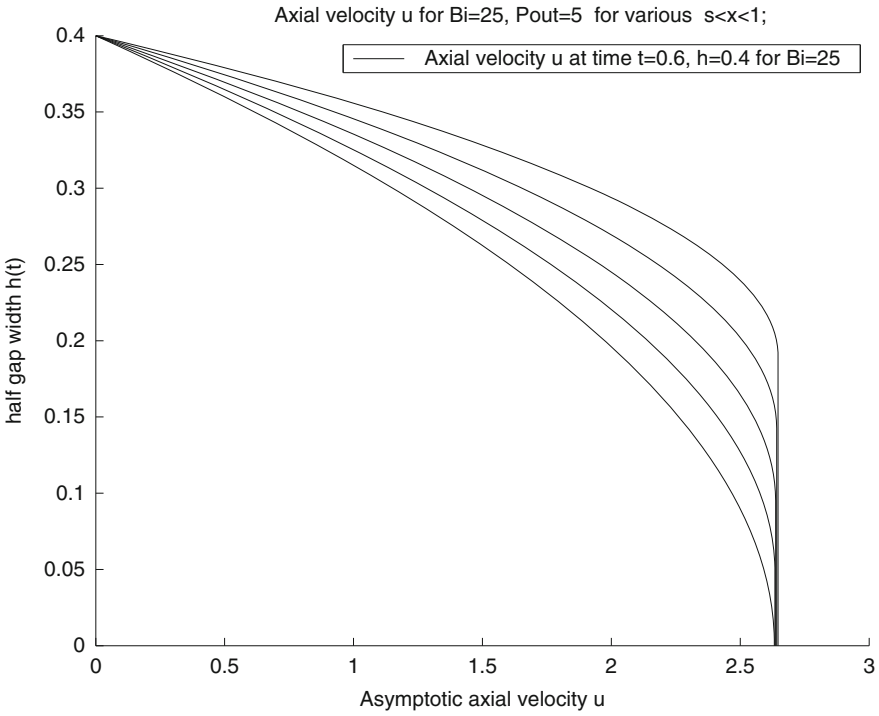

Fig. 30 u for $\mathsf{Bn} = 25$ and h given by (151)

with $A(t)$ to be determined. In $x \in [s, 1]$ we have

$$P_x(x,t) = -\frac{2u_p(t)}{(h-Y)^2},$$

so that

$$P_x = \frac{3}{h(s,t)\left[h(x,t) - Y(x,t)\right]^2} \int_0^s h_t d\xi, \tag{159}$$

with Y given by (156). We observe that (157) and (159) yield $P_x|_{s^-} = P_x|_{s^+}$. Let us now integrate (159) between x and 1 with the boundary condition $P(1,t) = P_{out}$. We find

$$P_{out} - P(x,t) = \frac{3}{h(s,t)} \int_0^s h_t d\xi \left[\int_x^1 \frac{d\tilde{x}}{\left(h(\tilde{x},t) - Y(\tilde{x},t)\right)^2} \right] \tag{160}$$

Imposing $P|_{s^-} = P|_{s^+}$, from (158), (160) we find $A(t)$, so that the pressure can be written in terms of s throughout the whole domain. Substituting (156) and (159)

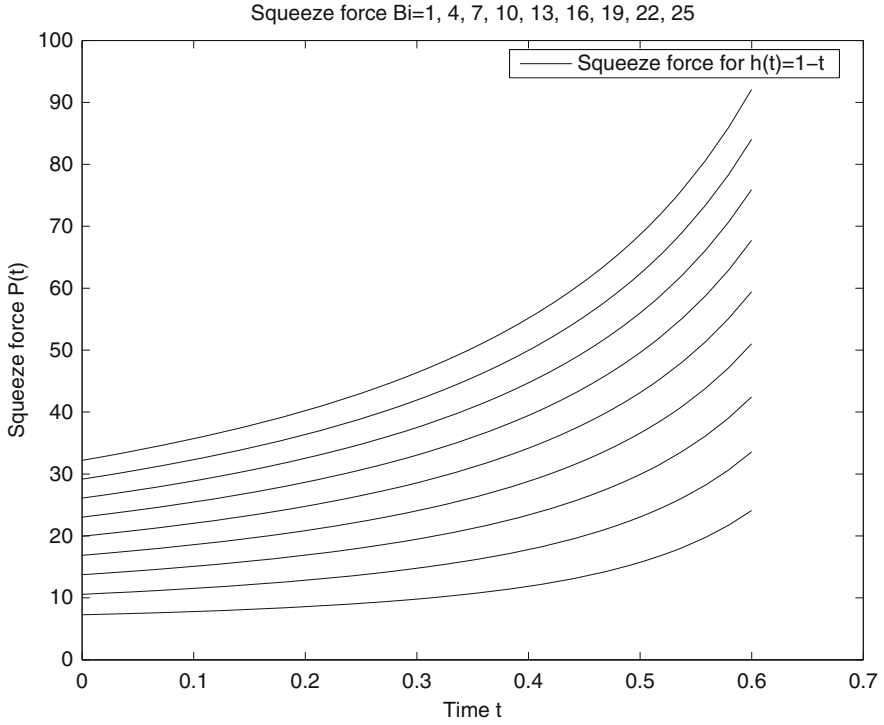

Fig. 31 Squeeze force for linear $h(t)$, (151)

into (140) we get

$$\int_s^1 \frac{\left[-2h(\tilde{x},t)+2h(s,t)\dfrac{\int_0^{\tilde{x}} h_t d\xi}{\int_0^s h_t d\xi}\right]_+}{\left[h(\tilde{x},t)-\left[-2h(\tilde{x},t)+2h(s,t)\dfrac{\int_0^{\tilde{x}} h_t d\xi}{\int_0^s h_t d\xi}\right]_+\right]^2} d\tilde{x} = -\frac{\mathrm{Bn}}{\left[\dfrac{3}{h(s,t)}\int_0^s h_t d\xi\right]}, \tag{161}$$

which provides an integral equation for the unknown $s(t)$. Equation (161) can be solved once we know the explicit form of the function $h(x,t)$.

When $h(x,t) = f(x)g(t)$, with $f \cdot g > 0$, then (161) can be rewritten as

$$\left(\int_0^s f d\xi\right)^2 \int_s^1 \frac{\left[-f(\tilde{x})\left(\int_0^s f d\xi\right)+f(s)\left(\int_0^{\tilde{x}} f d\xi\right)\right]_+ d\tilde{x}}{\left[\dfrac{f(\tilde{x})}{2}\left(\int_0^s f d\xi\right)-\left[-f(\tilde{x})\left(\int_0^s f d\xi\right)+f(s)\left(\int_0^{\tilde{x}} f d\xi\right)\right]_+\right]^2}$$
$$= -\frac{2\mathrm{Bn} f(s) g(t)^2}{3\dot{g}(t)}. \tag{162}$$

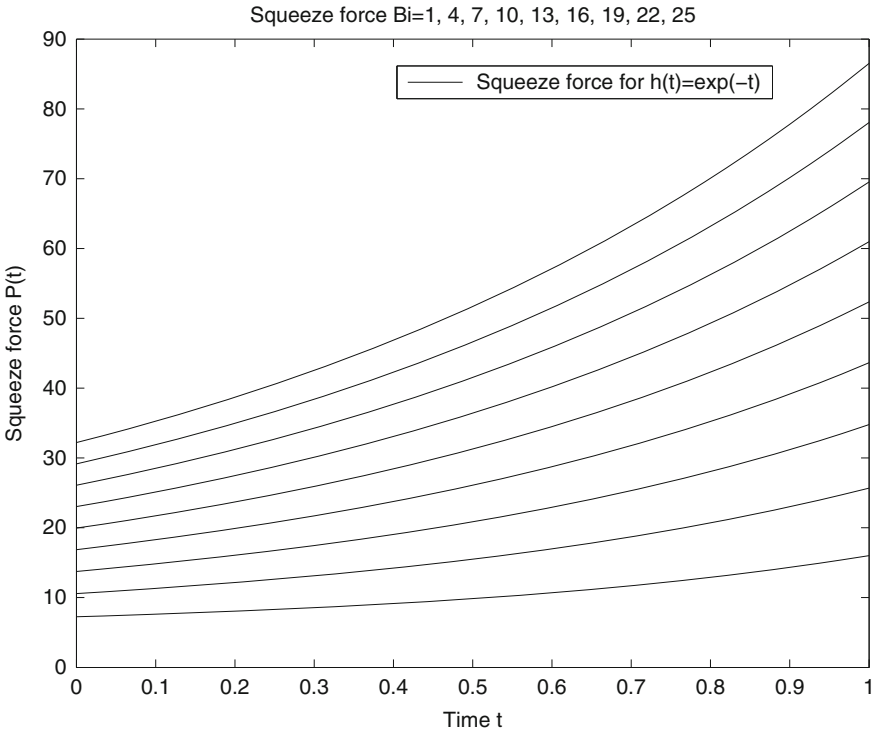

Fig. 32 Squeeze force for exponential $h(t)$, (152)

Example 7 Let us consider

$$h(x,t) = f(x)g(t), \quad \text{with} \quad f(x) = e^{-\beta x}, \quad g(t) = e^{-\alpha t},$$

where α, and β both positive. Exploiting (162) we find

$$\frac{4(1-e^{-\beta s})^2}{\beta}\int_s^1 \frac{(e^{-\beta s}-e^{-\beta x})}{\left[e^{-\beta x}(3-e^{-\beta s})-2e^{-\beta s}\right]^2}dx = \left(\frac{2\mathrm{Bn}}{3\alpha}\right)e^{-\beta s}e^{-\alpha t}. \tag{163}$$

or equivalently

$$\underbrace{\frac{(1-e^{-\beta s})^2}{\beta^2 e^{-2\beta s}}\left[\ln\frac{|2+e^{-\beta}-3e^{\beta(s-1)}|}{|e^{-\beta}-e^{\beta(s-1)}|}+\frac{2(e^{\beta(s-1)}-1)}{2+e^{-\beta}-3e^{\beta(s-1)}}\right]}_{\mathscr{G}(s)} = \left(\frac{2\mathrm{Bn}}{3\alpha}\right)e^{-\alpha t}, \tag{164}$$

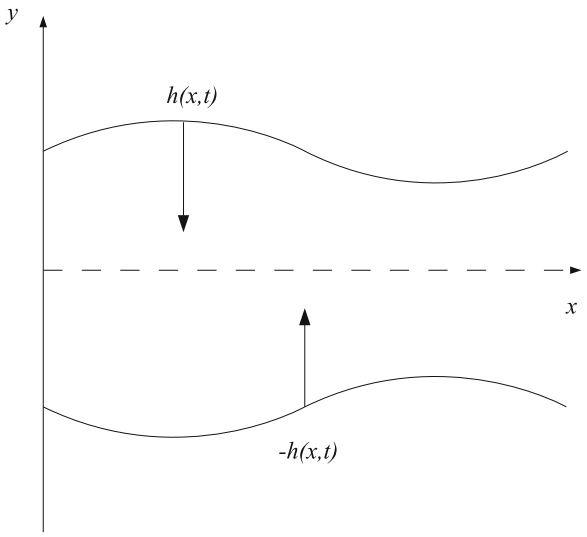

Fig. 33 A schematic representation of the squeezing channel

which is an implicit equation for $s(t)$. Notice that taking the limit $\beta \to 0$ of the l.h.s. of (164) we recover the l.h.s. of (149), as expected. We immediately realize that (164) admits a unique solution $s(t) \in (\hat{s}(\beta), 1]$, with

$$\hat{s}(\beta) = 1 + \frac{1}{\beta} \ln \left[\frac{e^{-\beta} + 2}{3} \right],$$

for each value of $(2\mathsf{Bn}/3\alpha)\, e^{-\alpha t}$. In particular it is easy to show that

$$\frac{2}{3} < \hat{s}(\beta) < 1, \qquad \forall \beta > 0,$$

so that $s \in (2/3, 1)$ for all $t > 0$. Recalling (156) we get

$$Y(x,t) = 2e^{-\alpha t} \left[\frac{e^{-\beta s} - e^{-\beta x}}{(1 - e^{-\beta s})} \right]. \tag{165}$$

Clearly $Y > 0$ for every $x > s$, and $Y = 0$ at $x = s$. Actually we can show that Y and h never meets. Indeed, suppose that $Y(x,t) < h(x,t)$, then

$$2 \left[\frac{e^{-\beta s} - e^{-\beta x}}{(1 - e^{-\beta s})} \right] < e^{-\beta x},$$

or analogously

$$2e^{\beta x} < 3e^{\beta s} - 1. \tag{166}$$

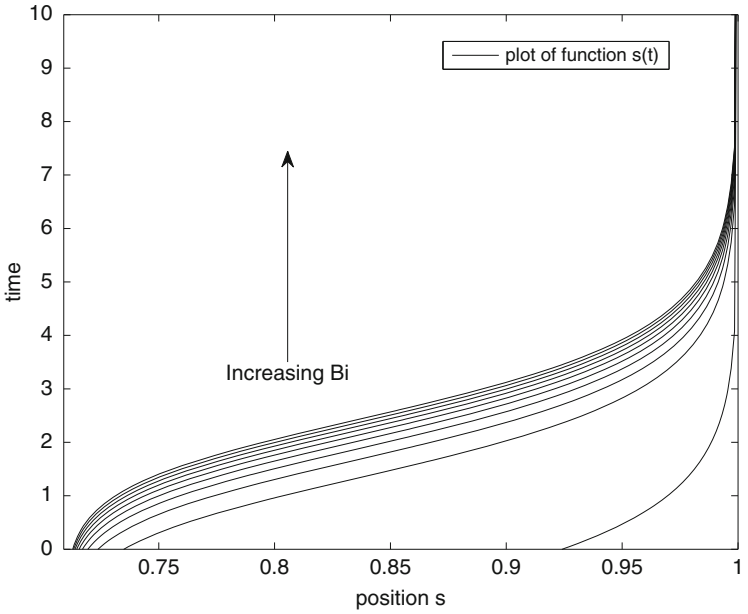

Fig. 34 The advance of the front $x = s(t)$ for Bn ranging between 0.1 and 100

Hence $Y < h$ if and only if (166) holds true for each $x \geq s$. Now recall that $s \geq \hat{s}(\beta) > 2/3$, for every finite time $t > 0$ and $\beta > 0$. Therefore

$$2e^{\beta x} \leq \max_{x\in[s,1]}\{2e^{\beta x}\} = 2e^{\beta} = 3e^{\beta\hat{s}} - 1 < 3e^{\beta s} - 1,$$

which proves that (166) holds true. As a consequence we get

$$0 \leq Y(x,t) < h(x,t), \quad \forall\ x \geq s, \quad t > 0.$$

We observe that $Y \to h$, which in turn tends to 0, only in the limit $t \to \infty$. In Fig. 34 we have plot the advancing front $x = s(t)$ for different values of Bn ranging from $\mathrm{Bn} = 0.1$ to $\mathrm{Bn} = 100$. The parameters used are $\alpha = 2$ and $\beta = 0.4$.

References

1. Bingham, E.C.: An investigation of the laws of plastic flow. U.S. Bur. Stand. Bull. **13**, 309–353 (1916)
2. Bingham, E.C.: Fluidity and Plasticity. McGraw Hill, New York (1922)
3. Coirier, J.: Mécanique des Milieux Continus. Dunod, Paris (1997)
4. Comparini, E.: A one-dimensional Bingham flow. J. Math. Anal. Appl. **169**, 127–139 (1992)

5. Coussot, P.: Yield stress fluid flows: a review of experimental data. J. Non-Newtonian Fluid Mech. **211**, 31–49 (2014)
6. Frigaard, I.A., Ryanb, D.P.: Flow of a visco-plastic fluid in a channel of slowly varying width. J. Non-Newtonian Fluid Mech. **123**, 67–83 (2004)
7. Fusi, L., Farina, A.: An extension of the Bingham model to the case of an elastic core. Adv. Math. Sci. Appl. **13**, 113–163 (2003)
8. Fusi, L., Farina, A.: A mathematical model for Bingham-like fluids with visco-elastic core. ZAMP **55**, 826–847 (2004)
9. Fusi, L., Farina, A.: Modelling of Bingham-like fluids with deformable core. Comput. Math. Appl. **53**, 583–594 (2007)
10. Fusi, L., Farina, A., Rosso, F.: Flow of a Bingham-like fluid in a finite channel of varying width: a two-scale approach. J. Non-Newtonian Fluid Mech. **177–178**, 76–88 (2012)
11. Fusi, L., Farina, A., Rosso F.: Retrieving the Bingham model from a bi-viscous model: some explanatory remarks. Appl. Math. Lett. **27**, 11–14 (2014)
12. Fusi, L., Farina, A., Rosso, F., Roscani, S.: Pressure driven lubrication flow of a Bingham fluid in a channel: a novel approach. J. Non-Newtonian Fluid Mech. **221** 66–75 (2015)
13. Hormozi, S., Dunbrack, G., Frigaard, I.A.: Visco-plastic sculpting. Phys. Fluids **26** (2014). http://dx.doi.org/10.1063/1.4894076
14. Huilgol, R.R.: Fluid Mechanics of Viscoplasticity. Springer, Berlin (2015)
15. Ionescu, I.R., Sofonea, M.: Functional and Numerical Methods in Viscoplasticity. Oxford University Press, Oxford (1993)
16. Joshi, S.C., Lam, Y.C., Boey, F.Y.C., Tok, A.I.Y.: Power law fluids and Bingham plastics flow models for ceramic tape casting. J. Materials Process. Technol. **120**, 215–225 (2002)
17. Lipscomb, G.G., Denn, M.M.: Flow of Bingham fluids in complex geometries. J. Non-Newtonian Fluid Mech. **14**, 337–346 (1984)
18. Liu, K., Mei, C.C.: Roll waves on a layer of a muddy fluid flowing down a gentle slope - a Bingham model. Phys. Fluids **6**, 2577–2590 (1994)
19. Muravleva, L.: Squeeze plane flow of viscoplastic Bingham material. J. Non-Newtonian Fluid Mech. **220**, 148–161 (2015)
20. Oldroyd, S.G.: A rational formulation of the equation of plastic flow for Bingham solid. Proc. Camb. Philos. Soc. **45**, 100–105 (1947)
21. Putz, A., Frigaard, I.A., Martinez, D.M.: On the lubrication paradox and the use of regularisation methods for lubrication flows. J. Non-Newtonian Fluid Mech. **163**, 62–77 (2009)
22. Rajagopal, K.R.: On implicit constitutive theories. Appl. Math. **48**, 279–319 (2003)
23. Rajagopal, K.R.: On implicit constitutive theories for fluids. J. Fluid Mech. **550**, 243–249 (2006)
24. Rajagopal, K.R., Srinivasa, A.R.: A thermodynamic frame work for rate type fluid models. J. Non-Newtonian Fluid Mech. **88**, 207–227 (2000)
25. Rajagopal, K.R., Srinivasa, A.R.: On the thermomechanics of materials that have multiple natural configurations Part I: viscoelasticity and classical plasticity. ZAMP **55**, 861–893 (2004)
26. Rajagopal, K.R., Srinivasa, A.R.: On the thermodynamics of fluids defined by implicit constitutive relations. ZAMP **59**, 715–729 (2008)
27. Roussel, N., Lanos, C.: Plastic fluid flow parameters identification using a simple squeezing test. Appl. Rheol. **13**, 132–141 (2003)
28. Rubinstein, L.I.: The Stefan Problem. Translations of Mathematical Monographs, vol. 27. American Mathematical Society, Providence, RI (1971)
29. Safronchik, A.I.: Nonstationary flow of a visco-plastic material between parallel walls. J. Appl. Math. Mech. **23**, 1314–1327 (1959)
30. Von Mises R., Mechanik der festen Körper im plastisch deformablen Zustand, Göttin. Nachr. Math. Phys. **1**, 582–592 (1913)
31. Wardhaugh, L.T., Boger, D.V.: Flow characteristics of waxy crude oils: application to pipeline design. AIChE J. **6**, 871–885 (1991)
32. Yoshimura, A.S., Prud'homme, R.K.: Response of an elastic Bingham fluid to oscillatory shear. Rheol. Acta **26**, 428–436 (1987)